

- [5] F.M. Boyce, N.L.R. Bucher, Baculovirus mediated gene transfer into mammalian cells, *Proc. Natl. Acad. Sci. USA* 93 (1996) 2348–2352.
- [6] V. Sandig, C. Hofmann, S. Steinert, G. Jennings, P. Schlag, M. Strauss, Gene transfer into hepatocytes and human liver tissue by baculovirus vectors, *Strauss, Hum. Gene Ther.* 7 (1996) 1937–1945.
- [7] I. Shoji, H. Aizaki, H. Tani, K. Ishihi, T. Chiba, I. Saito, T. Myamura, Y. Matsuura, Efficient gene transfer into various mammalian cells, including non-hepatic cells, by baculovirus vectors, *J. Gen. Virol.* 78 (1997) 2657–2664.
- [8] C.C. Yap, K. Ishii, Y. Aoki, H. Aizaki, H. Tani, H. Shimizu, Y. Ueno, T. Miyamura, Y. Matsuura, A hybrid baculovirus-T7 RNA polymerase system for recovery of infectious virus from cDNA, *Virology* 231 (1997) 192–200.
- [9] J.P. Condreay, S.M. Witherspoon, W.C. Clay, T.A. Kost, Transient and stable gene expression in mammalian cells transduced by a recombinant baculovirus vector, *Proc. Natl. Acad. Sci. USA* 96 (1999) 127–132.
- [10] C. Fipaldini, B. Bellei, N. La Monica, Expression of Hepatitis C virus cDNA in human hepatoma cell line mediated by a hybrid baculovirus-AAV vector, *Virology* 255 (1999) 302–311.
- [11] K.J. Airene, M.O. Hiltunen, M.P. Turunen, O.H. Laitinen, M.S. Kulomaa, Y.S. Herttuala, Baculovirus mediated periaortic gene transfer to rabbit carotid artery, *Gene Ther.* 7 (2000) 1499–1504.
- [12] C. Sarkis, C. Serguera, S. Petres, D. Buichet, J.L. Rider, L. Edelman, J. Mallet, Efficient transduction of neural cells in vitro and in vivo by a baculovirus-derived vector, *Proc. Natl. Acad. Sci. USA* 97 (2000) 14638–14643.
- [13] L. Pieroni, D. Maione, N. La Monica, In vivo gene transfer in mouse skeletal muscle mediated by baculovirus vectors, *Hum. Gene Ther.* 12 (2001) 871–881.
- [14] H. Tani, M. Mishijima, H. Ushijima, T. Miyamura, Y. Matsuura, Characterization of cell-surface determinants important for baculovirus infection, *Virology* 279 (2001) 343–353.
- [15] P. Lehtolainen, K. Tynnela, J. Kannasto, K.J. Airene, S. Yla-Herttuala, Baculovirus exhibits restricted cell type specificity in rat brain: a comparison of baculovirus-and adenovirus-mediated intracerebral gene transfer in vivo, *Gene Ther.* 9 (2002) 1693–1699.
- [16] H. Tani, C.K. Limn, C.C. Yap, M. Onishi, M. Nozaki, Y. Nishimune, N. Okahashi, Y. Kitagawa, R. Watanabe, R. Mochizuki, K. Moriishi, Y. Matsuura, In vitro and in vivo gene delivery by recombinant baculoviruses, *J. Virol.* 77 (2003) 9799–9808.
- [17] J. Barsoum, R. Brown, M. Mckee, F.M. Boyce, Efficient transduction of mammalian cells by a recombinant baculovirus having the vesicular stomatitis virus G glycoprotein, *Hum. Gene Ther.* 8 (1997) 2011–2018.
- [18] H. Aoki, Y. Sakoda, K. Jukuroki, A. Takada, H. Kida, A. Fukusho, Induction of antibodies in mice by a recombinant baculovirus expressing pseudorabies virus glycoprotein B in mammalian cells, *Vet. Microbiol.* 68 (1999) 197–207.
- [19] T. Abe, H. Takahashi, H. Hamazaki, N. Miyano-Kurosaki, Y. Matsuura, H. Takaku, Baculovirus induces an innate immune response and confers protection from lethal influenza virus infection in mice, *J. Immunol.* 171 (2003) 1133–1139.
- [20] L.J. Nicholson, M. Philippe, A.J. Paine, D.A. Mann, C.T. Dolphin, RNA interference mediated in human primary cells via recombinant baculoviral vectors, *Mol. Ther.* 11 (2005) 638–644.
- [21] S.-T. Ong, F. Li, J. Du, Y.-W. Tan, S. Wang, Hybrid cytomegalovirus enhancer-H1 promoter-based plasmid and baculovirus vectors mediate effective RNA interference, *Hum. Gen.* 16 (2005) 1404–1412.
- [22] L. Lu, Y. Ho, J. Kwang, Suppression of porcine arterivirus replication by baculovirus-delivered shRNA targeting nucleoprotein, *Biochem. Biophys. Res. Commun.* 340 (2006) 1178–1183.
- [23] S. Ghosh, M.K. Parvez, K. Banerjee, S.K. Sarin, E. Hasnain, Baculovirus as mammalian cell expression vector for gene therapy: an emerging strategy, *Mol. Ther.* 6 (2002) 5–11.
- [24] R. Gaynor, Cellular transcription factors involved in the regulation of HIV-1 gene expression, *AIDS* 6 (1992) 6347–6363.
- [25] A. el Kharroubi, E. Verdin, Protein-DNA interactions within DNase I-hypersensitive sites located downstream of the HIV-1 promoter, *J. Biol. Chem.* 269 (1994) 19916–19924.
- [26] K.A. Roebuck, D.S. Gu, M.F. Kagnoff, Activating protein-1 cooperates with phorbol ester activation signals to increase HIV-1 expression, *AIDS* 10 (1996) 819–826.
- [27] M.F. Rabbi, M. Saifuddin, D.S. Gu, M.F. Kagnoff, K.A. Roebuck, U5 region of the human immunodeficiency virus type 1 long terminal repeat contains TRE-like cAMP-responsive elements that bind both AP-1 and CREB/ATF proteins, *Virology* 233 (1997) 235–245.
- [28] C. Van Lint, C.A. Amella, S. Emiliani, M. John, T. Jie, E. Verdin, Transcription factor binding sites downstream of the human immunodeficiency virus type 1 transcription start site are important for virus infectivity, *J. Virol.* 71 (1997) 6113–6127.
- [29] Y. Habu, N. Miyano-Kurosaki, N. Matsumoto, H. Takeuchi, H. Takaku, Inhibition of HIV-1 replication by an HIV-1 dependent ribozyme expression vector with the Cre/loxP (ON/OFF) system, *Antivir. Chem. Chemother.* 13 (2002) 273–281.
- [30] G.W. Blissard, J.R. Wenz, Baculovirus GP64 envelope glycoprotein is sufficient to mediate pH dependent membrane fusion, *J. Virol.* 66 (1992) 6829–6835.
- [31] R.K. Akkina, R.M. Walton, M.L. Chen, Q.-X. Lim, V. Pannelles, I.S.Y. Chen, High-efficiency gene transfer into CD34<sup>+</sup> cells with a human immunodeficiency virus type 1-based retroviral vector pseudotyped with vesicular stomatitis virus envelope glycoprotein G, *J. Virol.* 70 (1996) 2581–2585.
- [32] J.D. Thompson, D.F. Ayers, T.A. Malmstorm, T.L. Mackenzie, L. Ganousis, B.M. Chowrira, L. Couture, D.T. Stinchcomb, Improved accumulation and activity of ribozymes expressed from a tRNA-based RNA polymerase III promoter, *Nucleic Acids Res.* 23 (1995) 2259–2268.
- [33] J. Barsoum, R. Brown, M. McKee, F.M. Boyce, Efficient transduction of mammalian cells by a recombinant baculovirus having the vesicular stomatitis virus G glycoprotein, *Hum. Gene Ther.* 8 (1997) 2011–2018.
- [34] S.-W. Park, H.-K. Lee, T.-G. Kim, S.-K. Yoon, S.-Y. Paik, Hepatocyte-specific gene expression by baculovirus pseudotyped with vesicular stomatitis virus envelope glycoprotein, *Biochem. Biophys. Res. Commun.* 289 (2001) 444–450.
- [35] A. Facciabene, J. Aurisicchio, N. La Monica, Baculovirus vector elicit antigen-specific immune responses in mice, *J. Virol.* 78 (2004) 8663–8672.
- [36] Y. Habu, N. Miyano-Kurosaki, M. Kitano, Y. Endo, M. Yukita, S. Ohira, H. Takaku, M. Nashimoto, H. Takaku, Inhibition of HIV-1 gene expression by retroviral vector-mediated small-guide RNAs that direct specific RNA cleavage by tRNase ZL, *Nucleic Acids Res.* 33 (2005) 235–243.
- [37] W.F. Anderson, Human gene therapy, *Science* 256 (1992) 808–813.
- [38] R.C. Mulligan, The basic science of gene therapy, *Science* 260 (1993) 926–932.
- [39] G.U. Dachs, G.J. Dougherty, I.J. Stratford, D.J. Chaplin, Targeting gene therapy to cancer, *Oncol. Res.* 9 (1997) 313–325.
- [40] C. Baum, H.G. Eckert, M. Stockschlader, U. Just, S. Hegewisch-Becker, M. Hildinger, A. Uhde, J. John, W. Ostertag, Improved retroviral vectors for hematopoietic stem cell protection and in vivo selection, *J. Hematother.* 5 (1996) 323–329.
- [41] C.E. Dunbar, J. Tisdale, J.M. Yu, T. Soma, T.J. Zujewski, D. Bodine, S. Sellers, K. Cowan, R. Donahue, R. Emmons, Transduction of hematopoietic stem cells in humans and in nonhuman primates, *Stem Cells* 1 (1997) 135–139.

## HIV gene therapy using RNA virus systems

Masaaki Hayafune<sup>1</sup>, Naoko Miyano-Kurosaki<sup>1,2</sup>, Akiko Kusunoki<sup>1</sup>, Yuka Mouri<sup>1</sup> and Hiroshi Takaku<sup>1,2</sup>

<sup>1</sup>Department of Life and Environmental Science and <sup>2</sup>High Technology Research Center, Chiba Institute of Technology, 2-17-1 Tsudanuma, Narashino, Chiba 275-0016, Japan

### ABSTRACT

We designed a vector to produce single-stranded DNA (ssDNA). We used HIV-1 reverse transcription for the purpose of constructing a DNAzyme expression vector against the HIV-1 env V3 loop. Initiation of HIV-1 reverse transcription requires the formation of a complex containing the viral RNA, tRNALys and reverse transcriptase. The expression vector contains the HIV-1 primer binding site (PBS) and tRNALys at the 3' end of its RNA transcript, thus enabling an ssDNA to be synthesized by HIV-1 reverse transcriptase. We have demonstrated that the DNAzyme expressed by the lentiviral vectors suppressed HIV-1 replication in SupT1 cells.

### INTRODUCTION

A DNAzyme (also known as deoxyribozyme, DNA enzyme) is a specifically structured DNA sequence that possesses catalytic RNA-cleaving activity, by recognizing its target RNA in a highly sequence-specific manner and blocking the expression of the corresponding RNA. mRNAs from oncogenes and viral genomes are ideal targets for DNAzyme therapeutic agents. A number of investigators have reported the sequence-specific cleavage of a variety of target RNAs, including HIV-1 RNA. The inhibition of infection by an incoming HIV-1 was reported by Zhang et al., who used DNAzymes that were targeted against the V3 loop of the envelope region<sup>1</sup>.

In our laboratory, Kusunoki et al. designed a vector for single-stranded DNA expression using HIV-1 RT<sup>2</sup>. The expressed DNAzyme had site-specific cleavage activity *in vitro*. In this study, we describe that a DNAzyme expression system transduced by a lentiviral vector, and assessed HIV-1 suppression in mammalian cells.

### MATERIALS AND METHODS

#### *Construction of lentiviral vectors.*

In order to construct the lentiviral vectors, the generated DNAzyme expression vectors<sup>2</sup> were digested with EcoR I, and then were cloned into the same site in the CS-CDF-CG-PRE vector<sup>3</sup>.

#### *Cell culture.*

293T and SupT1 cells were grown in RPMI 1640 medium or D-MEM (Sigma Aldrich) supplemented with 10%(v/v) heat-inactivated fetal bovine serum (FBS), penicillin (100 U/ml), streptomycin (100 µg/ml), and L-glutamine (2 mM). All cultures were maintained at 37°C under a 5% CO<sub>2</sub> atmosphere.

#### *RT-PCR analysis.*

Total RNA from vector-transfected cells was extracted with a GenElute Mammalian Total RNA kit (Sigma-Aldrich). RT-PCR was then performed using an RNA PCR high-plus kit (Toyobo) with env upstream (NL4-3 7070-7099), envneutral (NL4-3 7241-7271) and downstream (NL4-3 7570-7600) primers; these are referred to as forward primer F1- (5'-ACA GCT GAA CAC ATC TGT AGA AAT TAA TTG-3'), F2- (5'-AAA CAG ATA GCT AGC AAA TTA AGA GAA CAA-3') and reverse primer R1- (5'-GTT GTT ATT ACC ACC ATC TCT TGT TAA TAG-3'). These RT-PCR products were amplified using the following thermal cycle program: 1 cycle (60°C for 30 min and 94°C for 2 min), 25 cycles (94°C for 1 min and 51°C for 1.5 min), and 1 cycle (51°C for 7 min).

#### *Lentiviral vector preparation.*

A vector construct (15 µg) was co-transfected with the helper constructs encoding gag/pol (pMDLg/p.RRE) (15 µg), the rev expressing construct pRSV-rev (5 µg), and the VSV-G expressing construct pMD.G (5 µg), into 293T cells using the calcium phosphate-precipitation method. The supernatants were harvested 48h post-transfection, filtered through a 0.45 µm filter disc and concentrated 100-fold by centrifugation at 6,000g overnight. The resultant viral pellet was re-suspended in serum- and antibiotic-free RPMI medium and stored at -80°C until use. To determine the virus titer, SupT1 cells were transduced with the prepared viral stock, and the numbers of GFP-positive cells were assessed after 72h of culture by flow-cytometric analysis (Becton, Dickinson).

#### *Flow cytometry.*

Transduced SupT1 cells were washed twice in PBS, and then fixed in PBS containing 1% formaldehyde. Direct fluorescence of GFP was analyzed by a FACS Calibur system (Becton, Dickinson). Data acquisition and analysis were performed with the CellQuest software (Becton, Dickinson). Gates for GFP detection were established using mock-transduced cells as the background.

### HIV-1 challenge and culture assay.

After transduction by the lentiviral vectors, the GFP-positive SupT1 cells were sorted by a FACS vantage system (Becton, Dickinson), and were infected with HIV-1NL4-3 at an MOI of 0.01. After the harvested culture was centrifuged, the cell-free medium was used for an HIV-1 p24 CLEIA.

## RESULTS AND DISCUSSION

In order to express the DNAzyme targeted to HIV-1 (NL4-3 *env*: 7196-7210), we constructed three types of DNAzyme expression lentiviral vectors (CS-DZ-tRNA-0, CS-DZ-tRNA-1, CS-DZ-tRNA-2), which were under the control of the tRNA<sup>met</sup> promoter (Figure 1). As shown in Figure 1, we designed the tRNA<sup>Lys</sup> gene with three different lengths. Furthermore, we constructed an shRNA (NL4-3 *env*: 7193-7213) expression lentiviral vector (CS-env-shRNA).

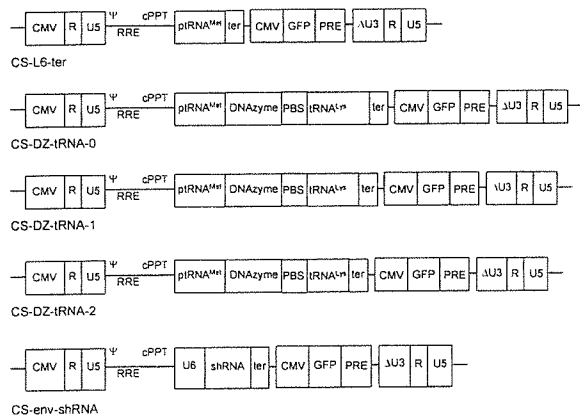


Figure 1. Construct of lentiviral vectors.

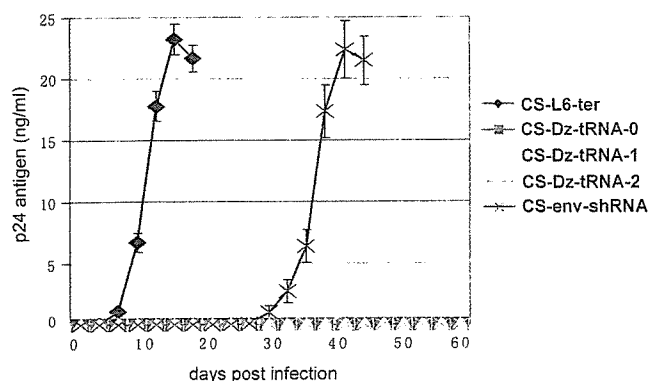


Figure 2. Inhibition of HIV-1 replication in SupT1 cells.

In order to investigate the sudden upsurge of viral replication, SupT1 cells were infected with the lentiviral vectors and wild-type HIV-1<sub>NL4-3</sub>, and the HIV-1 p24 antigen levels

were quantified in the cell-free supernatant (Figure 2). First, we observed the ssDNA expression under the above conditions (data not shown). Next, CS-DZ-tRNA-0, CS-DZ-tRNA-1 and CS-DZ-tRNA-2 were tested, and they almost completely suppressed HIV-1 replication. Although CS-env-shRNA had been almost completely suppress HIV-1 replication, after four weeks a mutation in the target site was observed. Furthermore, HIV-1 RNA cleavage by the DNAzyme and siRNA was examined by an RT-PCR analysis (Figure 3), which confirmed that HIV-1 RNA cleavage occurred in these transduced cells.

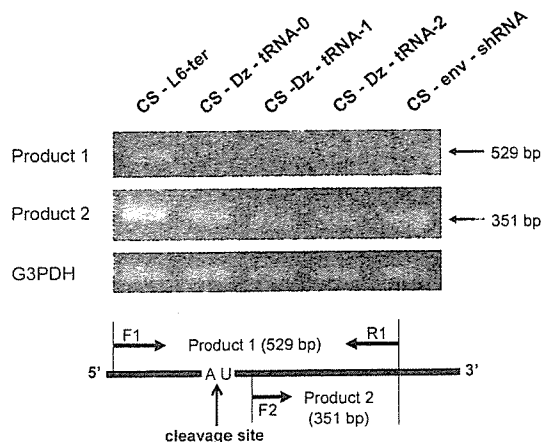


Figure 3. Confirmation of HIV-1 RNA cleavage.

## CONCLUSION

Our DNAzyme expression system was able to suppress HIV-1 replication for a relatively long period and was more effective than RNAi. Hence, this system might be an effective strategy for gene therapy applications in HIV-1/AIDS treatment.

## ACKNOWLEDGMENTS

This work was supported by a Grant-in-Aid for High Technology Research (HTR) from the Ministry of Education, Science, Sports, and Culture, Japan and by a Grant-in-Aid for AIDS research from the Ministry of Health, Labor, and Welfare, Japan (H17-AIDS-002).

## REFERENCES

- Zhang, X., Xu, Y., Ling, H., Hattori, T. (1999) *FEBES Lett.*, **458**, 151-156.
- Kusunoki, A., Miyano-Kurosaki, N., Takaku, H. (2003) *Biochem. Biophys. Res. Commun.*, **301**, 535-539.
- Naldini, L., Blomer, U., Gallay, P., Ory, D., Mulligan, R., Gage, F.H., Verma, I.M., Trono, D. (1996) *Science*, **272**, 263-267.

# Impaired GATA3-Dependent Chromatin Remodeling and Th2 Cell Differentiation Leading to Attenuated Allergic Airway Inflammation in Aging Mice<sup>1</sup>

Akihiro Hasegawa,\* Takako Miki,\* Hiroyuki Hosokawa,\* Mohammad B. Hossain,\* Chiori Shimizu,\* Kahoko Hashimoto,<sup>†</sup> Motoko Y. Kimura,\* Masakatsu Yamashita,\* and Toshinori Nakayama<sup>2\*</sup>

Age-related changes in lymphocytes are most prominent in the T cell compartment. There have been substantial numbers of reports on T cell function in aged mice and humans, such as on the production of Th1 and Th2 cytokines, but the results show considerable variation and contradictions. In the present study, we used 8- to 12-mo-old aging mice and a well-established in vitro Th1/Th2 cell differentiation culture system to identify molecular defects in Th1/Th2 cell differentiation that can be detected in the relatively early stages of aging. The capability to differentiate into Th2 cells is reduced in aging mouse CD4<sup>+</sup> T cells. Decreased activation of the ERK MAPK cascade upon TCR stimulation, but normal intracellular-free calcium ion concentration mobilization and normal IL-4-induced STAT6 activation were observed in aging mouse CD4<sup>+</sup> T cells. In addition, reduced expression of GATA3 was detected in developing Th2 cells. Chromatin remodeling of the Th2 cytokine gene locus was found to be impaired. Th2-dependent allergic airway inflammation was milder in aging mice compared with in young adult mice. These results suggest that the levels of Th2 cell differentiation and resulting Th2-dependent immune responses, including allergic airway inflammation, decline during aging through defects in the activation of the ERK MAPK cascade, expression of GATA3 protein and GATA3-dependent chromatin remodeling of the Th2 cytokine gene locus. In the present study, we provide the first evidence indicating that a chromatin-remodeling event in T cells is impaired by aging. *The Journal of Immunology*, 2006, 176: 2546–2554.

**T**he CD4<sup>+</sup> T cells consist of two distinct Th cell subpopulations, Th1 and Th2 cells (1). Th1 cells produce IFN- $\gamma$  and are involved in cell-mediated immunity against intracellular pathogens. Th2 cells produce IL-4, IL-5, and IL-13 and control humoral immunity and allergic reactions. Naive CD4<sup>+</sup> T cells differentiate into Th1 cells following recognition of Ags in the presence of IL-12, whereas IL-4 drives differentiation into Th2 cells (2–4). In addition to the cytokines mentioned above, TCR stimulation by Ags is also indispensable for both Th1 and Th2 cell differentiation. We reported that the efficient TCR-mediated activation of p56<sup>lck</sup>, calcineurin, and the Ras-ERK MAPK signaling cascade is required for Th2 cell differentiation (5–7). Several transcription factors that control Th1/Th2 cell differentiation have been identified (8, 9). Among them, GATA3 appears to be a master

transcription factor for Th2 cell differentiation (10–13) and Th2 cell maintenance (14, 15). Recently, we reported that the activation of the ERK MAPK cascade inhibits the ubiquitin-dependent degradation of GATA3 in developing Th2 cells and facilitates GATA3-dependent chromatin remodeling of the Th2 cytokine gene locus (16).

In the elderly, there is an increase in the frequency and severity of infectious diseases (17–19). Age-related changes in the immune system occur mainly in the T cell compartment (20–22). There may be related to a decrease in the ability of T cells to proliferate, and are associated with a reduction in IL-2 production (23) and reduced IL-2R expression (24–26). Various alterations in signaling have been described in comparison with young T cells. CD4<sup>+</sup> T cells from old mice show defects in TCR signal transduction that include diminished TCR- $\zeta$  phosphorylation, decreased elevation of intracellular Ca<sup>+</sup>, and diminished activation of the MEK/ERK pathway (20, 27, 28). In contrast, aging does not affect Zap70-TCR- $\zeta$  association (29).

T cells in the elderly are often characterized by a shift from naive to memory phenotypes (30, 31). The production of the type 1 cytokine IFN- $\gamma$  has been reported to be increased (32–34) or decreased (35–37) in aged mice and humans. Also, the production of type 2 cytokines such as IL-4 and IL-5 has been reported to be increased (38, 39) or decreased (33, 35) in vitro. These controversial observations on cytokine production may be a result of variations among the species or strains used in experiments, housing conditions or experimental culture systems. At present, age-related molecular defects in developing Th1/Th2 cells that control Th1/Th2 cytokine gene chromatin remodeling have not been formally investigated. In addition, it is not well clarified whether the severity of Th2-dependent allergic responses, such as allergic asthma, is modulated by aging.

\*Department of Immunology, Graduate School of Medicine, Chiba University, Chiba, Japan; and <sup>†</sup>Department of Life and Environmental Sciences and High Technology Research Center, Chiba Institute of Technology, Chiba, Japan

Received for publication August 19, 2005. Accepted for publication November 30, 2005.

The costs of publication of this article were defrayed in part by the payment of page charges. This article must therefore be hereby marked *advertisement* in accordance with 18 U.S.C. Section 1734 solely to indicate this fact.

<sup>1</sup> This work was supported by grants from the Ministry of Education, Culture, Sports, Science, and Technology (Japan) (Grants-in-Aid for Scientific Research, Priority Areas Research 17016010 and 17047007; Scientific Research B 17390139; Scientific Research C 16616003; Young Scientists 17790317 and 17790318, and Special Coordination Funds for Promoting Science and Technology), the Ministry of Health, Labor, and Welfare (Japan), the Program for Promotion of Fundamental Studies in Health Science of the National Institute of Biomedical Innovation, the Japan Health Science Foundation, Uehara Memorial Foundation, Kanoe Foundation, and the Mo-chida Memorial Foundation.

<sup>2</sup> Address correspondence and reprint request to Dr. Toshinori Nakayama, Department of Immunology, Graduate School of Medicine, Chiba University, 1-8-1 Inohana, Chuo-ku, Chiba 260-8670, Japan. E-mail address: tnakayama@faculty.chiba-u.jp

In the present study, we demonstrate that Th2 cell differentiation and Th2-dependent immune responses *in vivo*, including OVA-induced airway inflammation, are attenuated in aging mice. We detected several molecular defects in aging mouse CD4<sup>+</sup> T cells that may account for the attenuated Th2 responses. *i.e.*, 1) reduced activation of the ERK MAPK cascade upon TCR stimulation, 2) decreased GATA3 expression in developing Th2 cells, and 3) impaired chromatin remodeling of the Th2 cytokine gene locus.

## Materials and Methods

### Mice

C57BL/6 and BALB/c were purchased from Charles River Laboratories. All young adult (5–6 wk) and aging (8–12 mo) mice including OVA-specific TCR $\alpha\beta$  transgenic (DO.11.10 Tg) mice (40) used in this study were maintained under specific-pathogen-free conditions. Animal care was in accordance with the guidelines of Chiba University.

### Immunofluorescent staining and flow cytometric analysis

In general, 1 million cells were incubated on ice for 30 min with the appropriate staining reagents, according to a standard method (41). The reagents used in this study, anti-CD4-PE (RM4-1-PE), anti-CD4-FITC (RM4-1-FITC), anti-CD44-PE, anti-IL-4R $\alpha$  Ab, anti-CD25-FITC, and anti-CD69-FITC, were purchased from BD Pharmingen. Anti-rat Ig-FITC was purchased from CAPPEL. Anti-TCR $\beta$ -FITC (H57-FITC), anti-TCR $\beta$ -biotin, and anti-CD3-FITC (2C11-FITC) were prepared in our laboratory. Flow cytometric analysis was performed on a FACSCalibur (BD Biosciences), and the results were analyzed with CellQuest software (BD Biosciences). Intracellular staining of IL-4 and IFN- $\gamma$  was performed as described previously (6). FITC- or allophycocyanin-conjugated anti-IFN- $\gamma$  Ab (XMG1.2; BD Pharmingen) and PE- or allophycocyanin-conjugated anti-IL-4 Ab (11B11; BD Pharmingen) were used for detection.

### Cell purification

Splenic CD4<sup>+</sup> T cells were stained with anti-CD4-FITC and then purified using anti-FITC magnetic beads (Miltenyi Biotec) and an AutoMACS sorter (Miltenyi Biotec), yielding a purity of >98%. In some experiments, spleen cells were stained with anti-CD4 and anti-CD44, and naive CD4<sup>+</sup>CD44<sup>low</sup> T cells were sorted by a FACS Vantage (BD Biosciences) and used as responder T cells as described previously (42).

### Proliferation assay

Splenic CD4<sup>+</sup> T cells ( $2 \times 10^5$ ) prepared by the AutoMACS sorter were stimulated in 200- $\mu$ l cultures for 40 h with immobilized anti-TCR $\beta$  mAb (H57-597). [<sup>3</sup>H]Thymidine (37 kBq/well) was added to the stimulation culture for the last 16 h, and the incorporated radioactivity was measured on a beta plate (6).

### Analysis of the efficiency of cell division

Splenic CD4<sup>+</sup> T cells purified by the AutoMACS sorter were labeled with CFSE (Molecular Probes) as described previously (42).

### Measurement of intracellular-free calcium ion concentration ([Ca<sup>2+</sup>]<sub>i</sub>)<sup>3</sup>

Splenic CD4<sup>+</sup> T cells purified by the AutoMACS sorter were loaded with Indo-1 (Indo-1 AM; Molecular Probes) in the presence of F127 (41). After washing, the cells were incubated with anti-CD4-FITC and anti-TCR $\beta$ -biotin on ice. The stained cells were washed and subjected to Ca analysis on a FACS Vantage (BD Biosciences). TCR was cross-linked with avidin, the [Ca<sup>2+</sup>]<sub>i</sub> was monitored for 512 s, and the results were analyzed with CellQuest software (BD Biosciences).

### In vitro Th1/Th2 cell differentiation cultures

DO11.10 Tg CD44<sup>low</sup>CD4<sup>+</sup> T cells ( $1.5 \times 10^4$ ) purified by cell sorting were stimulated with antigenic OVA peptide (OVA; 323–339, 10  $\mu$ M) and irradiated (3000 rad) BALB/c APCs ( $1 \times 10^5$ ) in the presence of exogenous IL-4 or IL-12 as described previously (6).

### ELISA for the measurement of cytokine concentration

The productions of IL-2, IL-4, IL-5, IL-13, and IFN- $\gamma$  were measured by ELISA as described previously (43).

### RT-PCR analysis

The quantitative RT-PCR analysis of GATA3 expression was performed as described previously (44).

### Retroviral vectors and infection

cDNA for human GATA3 was inserted into a multicloning site of pMX-IRES-GFP (16). The methods for the generation of the virus supernatant and infection were described previously (16).

### OVA immunization and ELISA for the measurement of serum Ig concentration

Young (6 wk old) and old (10 mo old) BALB/c mice were immunized *i.p.* with 100  $\mu$ g of OVA emulsified in CFA (Difco) on days 0 and 7. Blood was collected from the tail vein on day 14. The concentrations of IgE in the serum were measured with a mouse IgE ELISA kit (BD Biosciences). The concentrations of OVA-specific Igs (IgG1 and IgG2a) in the serum were determined by ELISA as described previously (5).

### Immunoblotting

Immunoblotting was performed as described previously (6). For ERK1 and ERK2 phosphorylation, naive CD4<sup>+</sup> T cells from C57BL/6 mice were purified with anti-CD4 mAb (RM4-5) and magnetic beads sorting (MACS sorting), and then the cells were incubated with anti-TCR mAb (H57-597) on ice. After incubation, the cells were stimulated with anti-hamster Igs (which cross-reacts with both H57-597) for 3, 10, or 30 min at 37°C, and then total cell lysates were subjected to phospho-ERK immunoblotting (Cell Signaling Technology). For STAT6 phosphorylation, naive CD4<sup>+</sup> T cells from C57BL/6 mice were activated with immobilized anti-TCR mAb and IL-4 (100 U/ml) for 2 days (induction culture). To assess IL-4-induced tyrosine phosphorylation, stimulated cells were washed, cultured for 8 h without cytokines, and stimulated with IL-4 (100 U/ml) for 3, 10, 30, or 60 min at 37°C. For IL-4 titration, 10–100 U/ml IL-4 was used. Anti-phosphotyrosine (RC20; BD Transduction Laboratories) or antiserum reactive with STAT6 (R&D Systems) was used for detection. For the detection of GATA3 or JunB, nuclear extracts were prepared with NE-PER Nuclear and Cytoplasmic Extraction Reagent (Pierce) according to the manufacturer's protocol. Immunoblotting was performed with anti-GATA3 mAb or anti-JunB mAb (Santa Cruz Biotechnology). HRP-conjugated anti-mouse Ig Ab (Amersham Biosciences) was used for GATA3 or JunB visualization (45).

### Chromatin immunoprecipitation (ChIP) assay

Acetylation status of histone H3-K9/K4 was assessed using histone H3 (K9/14) ChIP assay kits (no. 17-245; Upstate Biotechnology) as described previously (46). The ChIP assay for di-methylated histone H3-K4 was performed using anti-histone H3 dimethyl K4 antiserum (no. 07-030; Upstate Biotechnology) (47). Semiquantitative PCR was performed with DNA samples from  $3 \times 10^4$  or  $1 \times 10^4$  cells at 28 cycles. PCR products were resolved in an agarose gel and visualized and quantified using an ATTO L&S analyzer (ATTO). The primers used were described previously (46).

### Sensitization and inhalation with OVA

Young (6 wk old) and old (12 mo old) BALB/c mice were immunized *i.p.* with 250  $\mu$ g of OVA (chicken egg albumin purchased from Sigma-Aldrich) in 4 mg of aluminum hydroxide gel (alum) on days 0 and 7. Mice were made to inhale aerosolized OVA in saline (10 mg/ml) for 30 min using a supersonic nebulizer (model NE-U07; Omron) on days 14 and 16 to assess eosinophilic inflammation as described previously (48).

### Collection of bronchioalveolar lavage (BAL) fluid and lung histology

Two days after the last OVA inhalation on day 16, BAL was performed as described previously (49). Total BAL fluid was collected and the cells in 100- $\mu$ l aliquots were counted. One hundred thousand viable BAL cells were cytocentrifuged onto slides using a Cytospin3 (Thermo Shandon) and stained with May-Grünwald-Giemsa solution (Merck) as described previously (50). Two hundred leukocytes were counted on each slide. Cell types were identified using morphological criteria. The percentages of each cell type were calculated.

<sup>3</sup> Abbreviations used in this paper: [Ca<sup>2+</sup>]<sub>i</sub>, free calcium ion concentration; ChIP, chromatin immunoprecipitation; BAL, bronchioalveolar lavage.

For lung histology, mice were sacrificed by CO<sub>2</sub> asphyxiation 48 h after the last OVA inhalation on day 16, and the lungs were infused with 10% (v/v) Formalin in PBS for fixation. The lung samples were sectioned, stained with H&E reagents, and examined for pathological changes under a light microscope at  $\times 200$ . Numbers of infiltrated mononuclear cells in the perivascular and peribronchiolar regions were enumerated by direct counting of four different fields per slide as described previously (51).

## Results

### Phenotypic and functional characterization of aging mouse CD4<sup>+</sup> T cells

We initiated the analysis of T cells of aging C57BL/6 mice (8–12 mo) maintained under specific pathogen-free conditions by examining the expression of cell surface molecules on splenic CD4<sup>+</sup> T cells. Representative CD4/CD8 profiles for young and aging mice are shown in Fig. 1A. The yields of spleen cells were  $112 \pm 24 \times 10^6$  ( $n = 8$ ) for young mice and  $134 \pm 34 \times 10^6$  ( $n = 8$ ) for aging mice. The percentages of CD4<sup>+</sup> and CD8<sup>+</sup> T cells in the spleen were similar between young and aging mice, and the cell surface expression of TCR $\alpha\beta$  and CD3 on the splenic CD4<sup>+</sup> T cells was also similar (Fig. 1B). However, the numbers of CD25<sup>+</sup> cells, CD69<sup>+</sup> cells, and memory type (CD44<sup>high</sup>) CD4<sup>+</sup> T cells in aging mice were higher than in young mice. The expression level of IL-4R $\alpha$  on CD4<sup>+</sup> T cells was slightly higher in aging mice. As for T cell function, the anti-TCR $\beta$  mAb-induced proliferative responses of CD4<sup>+</sup> T cells were lower in aging mice (Fig. 1C). We examined the anti-TCR-induced cell division of CD4<sup>+</sup> T cells in Th1- or Th2-skewed differentiation cultures and found that CFSE-labeled naive CD4<sup>+</sup> T cells were stimulated by the anti-TCR $\beta$  mAb in the presence of IL-2 and IL-12 (Th1 culture conditions) or IL-2 and IL-4 (Th2 culture conditions). After 72 h of culture, the cells had divided three to four times in the case of both young and aging mouse T cells. The rate of cell division of aging mouse CD4<sup>+</sup> T cells was slightly impaired under either Th1- or Th2-skewed conditions (Fig. 1D). Similar results were obtained using CD4<sup>+</sup> T cells from BALB/c mice (data not shown). These results suggest that CD4<sup>+</sup> T cells from aging mice have a moderately decreased proliferative response to anti-TCR stimulation, a finding consistent with previous reports (17, 18).

### In vitro Th1/Th2 cell differentiation of naive CD4<sup>+</sup> T cells from aging mice

Th1/Th2 cell differentiation of naive CD4<sup>+</sup> T cells from young and aging mice was examined using a well-established in vitro culture system (5). Naive CD4<sup>+</sup> T cells from aging OVA-specific TCR $\alpha\beta$  Tg (DO11.10 Tg) mice were sorted and stimulated with antigenic OVA peptide in the presence of young BALB/c APCs for 5 days. CD4<sup>+</sup> T cells from young DO11.10 Tg mice preferentially differentiated into IL-4-producing Th2 cells in an Ag dose-dependent fashion (Fig. 2, left upper panels). However, for aging mice, the generation of Th2 cells was decreased, and a significant increase in the number of IFN- $\gamma$ -producing Th1 T cells was observed (Fig. 2, left panels). The levels of Th2 cell differentiation induced by a minimal dose of antigenic peptide (0.1  $\mu$ M), and exogenous IL-4 was also decreased in old DO11.10 Tg T cell cultures (Fig. 2, middle panels). In contrast, the IL-12-dependent induction of Th1 cell differentiation remained intact (Fig. 2, right panels). These results suggest that the efficiency of Th2 cell differentiation is reduced in aging mice.

### Anti-TCR-induced cytokine production profiles of splenic CD4<sup>+</sup> T cells from aging mice

Purified BALB/c CD4<sup>+</sup> T cells from young and aging mice were stimulated in vitro with immobilized anti-TCR $\beta$  mAb, and the level of cytokines in the culture supernatant was determined by

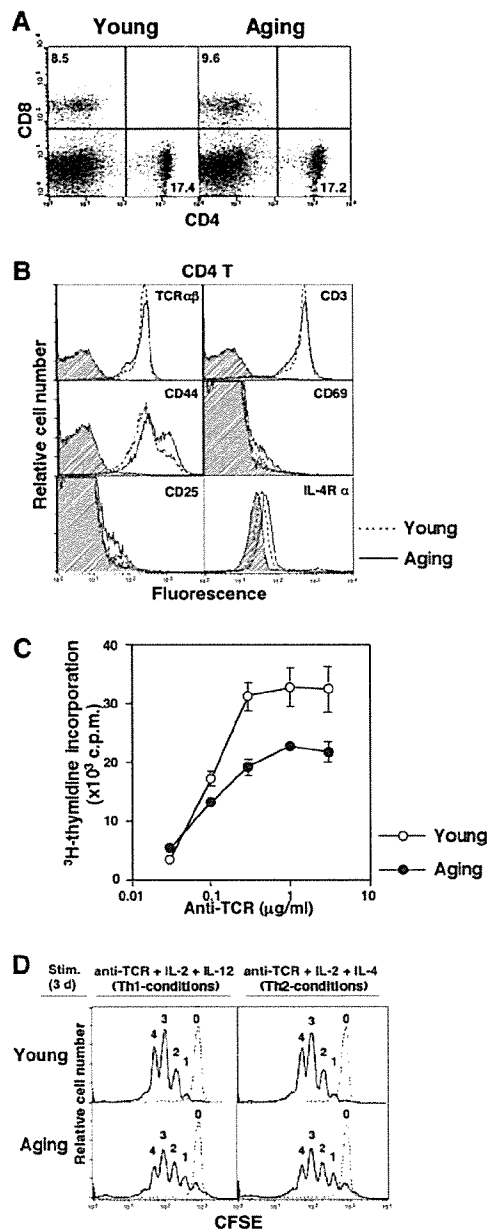


**FIGURE 1.** Phenotypic and functional characterization of aging mouse T cells. *A*, Representative CD4/CD8 profiles of splenocytes of young (6 wk old) and aging (9 mo old) C57BL/6 mice are shown. Percentages of cells present in each area are also shown. *B*, Each histogram depicts the expression of the indicated marker Ags on electronically gated splenic CD4<sup>+</sup> T cells from young (dotted lines) and aging (solid lines) mice. Background staining is shown as hatched areas. *C*, Splenic CD4<sup>+</sup> T cells from young (○) and aging (●) mice were stimulated with immobilized anti-TCR $\beta$  mAb. The mean [<sup>3</sup>H]thymidine incorporation of each group is shown with SDs. *D*, Naive CD4<sup>+</sup> T cells were labeled with CFSE and stimulated with immobilized anti-TCR $\beta$  mAb under Th1- or Th2-skewed conditions. After 3 days of culture, the number of cell divisions (0 to 4) was assessed by flow cytometry.

ELISA (Fig. 3). The levels of IL-2 were not obviously decreased on day 2 but decreased on day 3. The production of IFN- $\gamma$  in aging mouse CD4<sup>+</sup> T cell cultures was substantially increased on day 5 and day 7. In contrast, the levels of all Th2 cytokines, IL-4, IL-5, and IL-13, in aging mouse T cell cultures were decreased on days

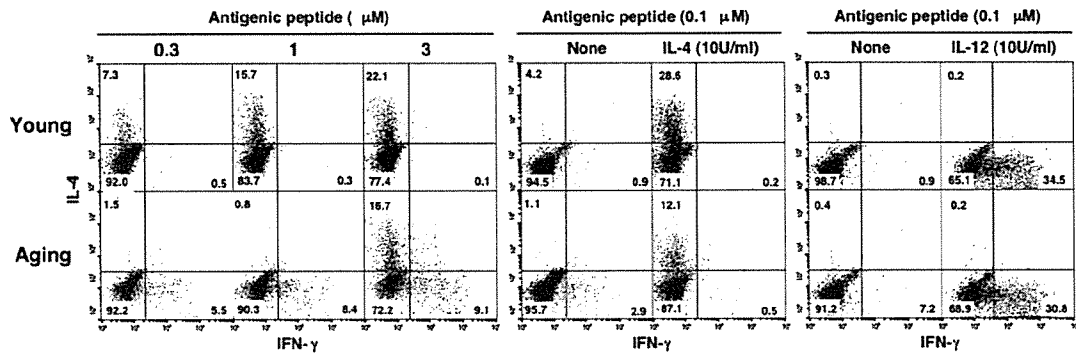


**FIGURE 2.** In vitro Th1/Th2 cell differentiation of naive CD4<sup>+</sup> T cells from aging mice. Naive (CD44<sup>low</sup>) CD4<sup>+</sup> T cells purified by cell sorting from the spleens of aging OVA-specific TCRαβ Tg (DO11.10 Tg) mice were stimulated with the indicated doses of antigenic peptide (OVA; 323–339) and irradiated young BALB/c APCs (*left panel*), a minimal dose of peptide (0.1 μM) and APCs in the presence of exogenous IL-4 (*middle panel*) or IL-12 and anti-IL-4 mAb (*right panel*) for 5 days. Intracellular staining profiles of IFN-γ and IL-4 are shown with percentages of cells in each area. The results are representative of five experiments.

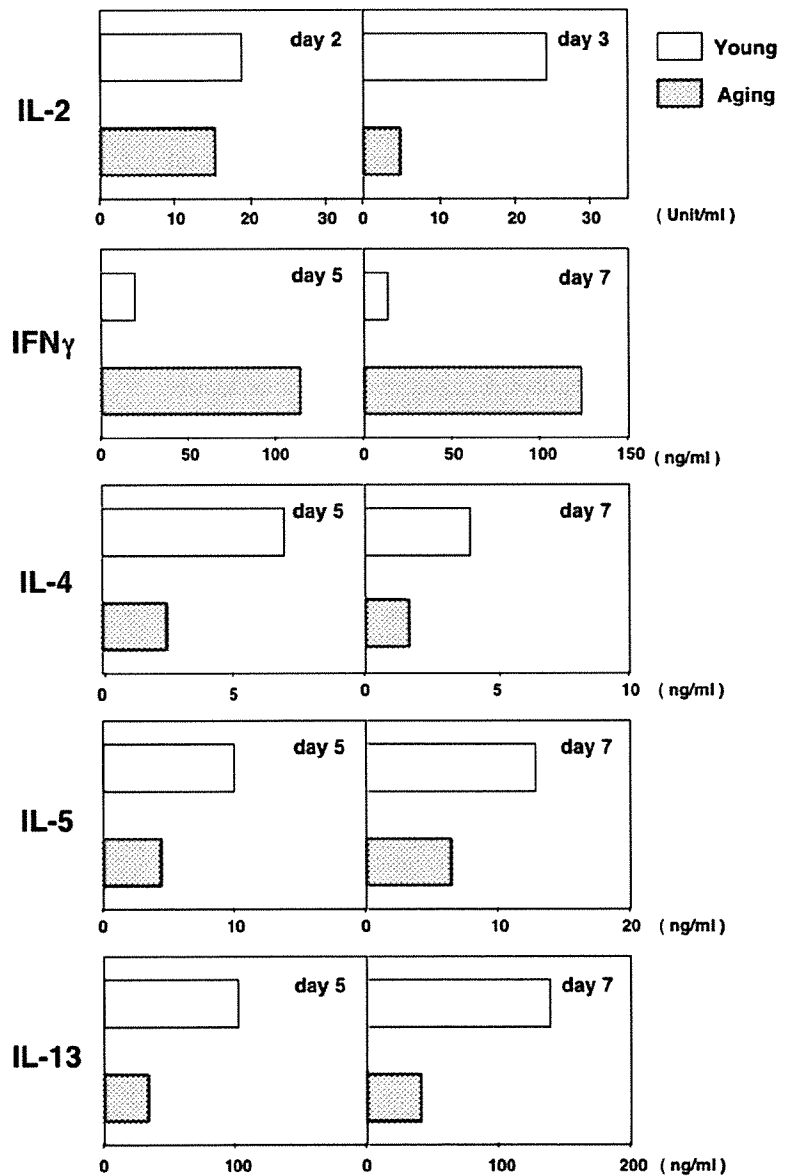


**FIGURE 3.** Decreased Th2 cytokine production in aging mouse CD4<sup>+</sup> T cells. Purified BALB/c splenic CD4<sup>+</sup> T cells were stimulated with immobilized anti-TCRβ mAb for 2 and 3 days (IL-2), or 5 and 7 days (IL-4, IL-5, IL-13, and IFN-γ). The concentration of cytokines in the culture supernatant was determined by ELISA. Three independent experiments were performed with similar results.

5 and 7. Similar cytokine production profiles were obtained in the anti-CD3 stimulation cultures (data not shown).

#### Th1/Th2-dependent Ab production in aging mice

Th2 cells play an important role in the stimulation of B cells to produce high levels of Ag-specific IgG1 and IgE in vivo, whereas the IgG2a isotype is a consequence of the generation of Th1 cells. Young and aging BALB/c mice were immunized with OVA-CFA, and the serum concentrations of total IgE, OVA-specific IgG1 and IgG2a were measured. As expected, the serum concentration of total IgE was significantly decreased in aging mice (Fig. 4, *left panel*). The serum concentration of IgG1 was significantly lower in aging mice (Fig. 4, *middle panel*), while Th1-dependent OVA-specific IgG2a levels were not decreased (Fig. 4, *right panel*). The production of Ag-specific IgE was not detected (data not shown). These results suggest that Th2-dependent Ab responses in vivo are decreased in aging mice preserving Th1 responses intact.

#### Signal transduction downstream of IL-4R in CD4<sup>+</sup> T cells from aging mice

To assess the activation of the IL-4R signaling pathway, freshly prepared CD4<sup>+</sup> T cells from young and aging mice were stimulated with IL-4, and then the tyrosine phosphorylation of STAT6 was examined. No significant differences in the magnitude or time course of phosphorylation of STAT6 were observed (Fig. 5A). Protein expression of STAT6 was comparable between young and old mice. Moreover, STAT6 phosphorylation induced by various doses of IL-4 was also comparable (Fig. 5B). Thus, the IL-4R signaling cascade appears to be intact in CD4<sup>+</sup> T cells from aging mice.

#### Signal transduction through TCR in CD4<sup>+</sup> T cells from aging mice

Next, we assessed the levels of signaling activation downstream of TCR. First, [Ca<sup>2+</sup>]<sub>i</sub> mobilization in CD4<sup>+</sup> T cells was assessed after TCR cross-linking, and a slightly higher percentages of responding cells and slightly higher magnitude of the response were observed (Fig. 5C). Next, naive CD4<sup>+</sup> T cells from young and aging mice were stimulated with anti-TCR mAb, and the tyrosine phosphorylation of ERK1 and ERK2, reflecting MAPKK activation, was examined (Fig. 5D). Although the expression levels of ERK1 and ERK2 protein were comparable, the levels of phosphorylation of both ERK1 and ERK2 were reduced substantially in CD4<sup>+</sup> T cells from aging mice. The background phosphorylation was also slightly reduced (see time 0). These results suggest that the activation of the Ras-ERK MAPK cascade is impaired in aging mouse CD4<sup>+</sup> T cells.

#### Decreased GATA3 induction in CD4<sup>+</sup> T cells differentiated under Th2 culture conditions

Because the levels of GATA3 and JunB expression are reported to be critical for Th2 cell differentiation (11), we assessed the protein and mRNA expression levels of GATA3 and JunB in developing Th2 cells. Naive CD4<sup>+</sup> T cells from young and aging BALB/c mice were stimulated with anti-TCRβ mAb in the presence of IL-4 and anti-IL-12 mAb for 5 days, and the protein expression levels of GATA3, JunB, and tubulin-α (Fig. 6A), and the mRNA expression levels of GATA3 (Fig. 6B) were assessed. The levels of GATA3 protein were decreased substantially in aging mouse CD4<sup>+</sup> T cells, while the levels of JunB were unchanged. Regarding the GATA3 mRNA levels, the decrease was significant but less dramatic in aging mouse T cells. These results suggest that GATA3 induction is significantly impaired in developing Th2 cells of aging mice.

In an attempt to rescue the inefficient Th2 cell differentiation in aging mouse T cells, we introduced GATA3 by retrovirus infection into aging mouse developing Th2 cells on day 2 of Th1/Th2 cell differentiation culture, and the generation of Th1/Th2 cells was assessed on day 5 (Fig. 6C). Although not complete, a substantial rescue of Th2 cell generation was observed. These results suggest that the inefficient Th2 cell differentiation in aging mouse T cells is due, at least in part, to the decreased expression of GATA3.

#### Chromatin remodeling of the Th2 cytokine gene locus in CD4<sup>+</sup> T cells from aging mice

We reported that Th2 responses are highly dependent on the extent of activation of the Ras-ERK MAPK cascade (6, 48). The hyperacetylation of histones associated with the Th2 cytokine gene locus is dependent on the expression of GATA3 (43, 46). Activation of the ERK-MAPK cascade is required for GATA3-dependent histone H3 hyperacetylation of the Th2 cytokine gene locus (16). Consequently, we wished to examine the chromatin remodeling of the Th2 cytokine gene locus in CD4<sup>+</sup> T cells from aging mice. The acetylation levels of histones associated with the Th2 cytokine gene locus (IL-4 promoter, IL-5 promoter, and IL-13 promoter) were reduced significantly in Th2 cells from aging mice (Fig. 7, A and B). The acetylation of the CNS1 region was reduced slightly in aging mouse Th2 cells. Similarly, the methylation levels of histones associated with the Th2 cytokine gene locus (IL-4 promoter, IL-5 promoter, and IL-13 promoter) and CNS1 region were significantly reduced in Th2 cells from aging mice (Fig. 7, A and C). These results indicate that histone H3 hyperacetylation and methylation of the Th2 cytokine gene locus are significantly decreased in developing Th2 cells of aging mice.

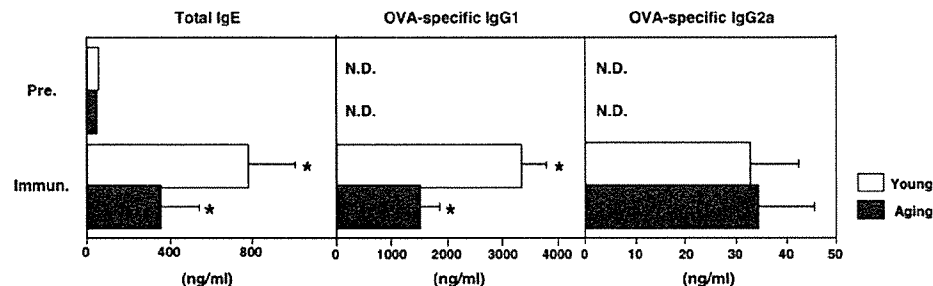
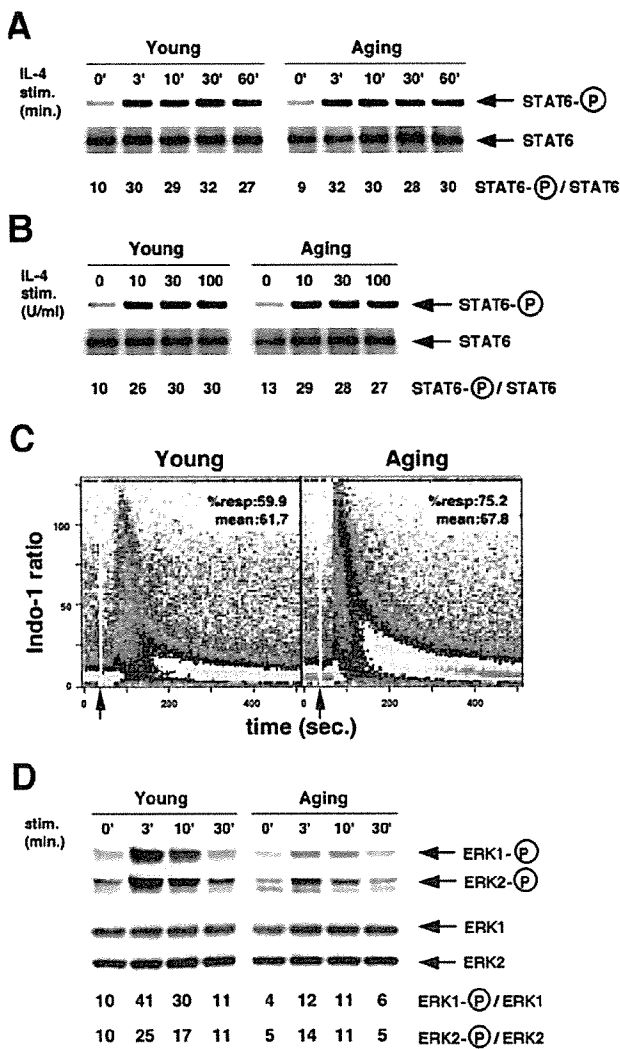
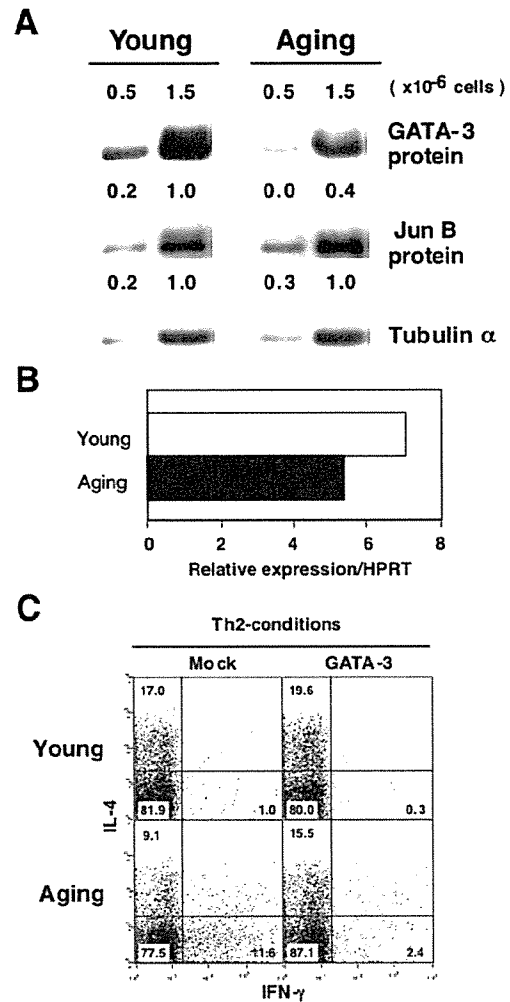


FIGURE 4. Th1/Th2-dependent immune responses in aging mice. Young (6 wk old) and aging (9 mo old) BALB/c mice (five mice per group) were immunized with OVA with CFA. Two weeks later, mean concentrations of total IgE and OVA-specific IgG1 and IgG2a Abs in the serum were determined. Data are shown with SEM. \*,  $p < 0.05$  by Student's  $t$  test. N.D., not detected.





**FIGURE 5.** Signal transduction through TCR or IL-4R in CD4<sup>+</sup> T cells from young and aging mice. *A* and *B*, Naive CD4<sup>+</sup> T cells from young and aging mice were cultured for 2 days with immobilized anti-TCR mAb and IL-4, cultured without IL-4 for 8 h, and then the IL-4-induced phosphorylation on STAT6 (3–60 min with 100 U/ml IL-4 in *A*; 10 min with 10–100 U/ml IL-4 in *B*) was assessed by immunoprecipitation and immunoblotting with anti-phosphotyrosine mAb. The amount of STAT6 protein was also determined by reblotting the same membrane with specific mAbs. Arbitrary densitometric ratios (phospho-STAT6/STAT6) are shown under each band. Four independent experiments were done with similar results. *C*, Intracellular-free calcium ion levels after TCR-cross-linking (arrows) were measured by flow cytometric analysis of Indo-1-labeled naive CD4<sup>+</sup> T cells from young and aging mice. The mean ratio of violet to blue fluorescence of Indo-1 is plotted vs time following stimulation. Shown are data obtained by gating electronically on CD4<sup>+</sup> T cells. The percentages of responding cells and the mean response (ratio) of the responding cells are also shown. *D*, TCR-induced MAPKK activation in splenic CD4<sup>+</sup> T cells from aging mice. The phosphorylation status of ERK1 and ERK2 in splenic CD4<sup>+</sup> T cells was assessed 3–30 min after TCR cross-linking. After stimulation, the cells were lysed, and the lysates were subjected to immunoblotting with anti-phospho-ERK or anti-ERK Abs. Densitometric measurements of the phosphorylated bands (p44 for ERK1 and p42 for ERK2) are shown under each band in arbitrary units. Three independent experiments were done with similar results.



**FIGURE 6.** GATA3 expression and the effect of overexpression of GATA3 in developing Th2 cells from aging mice. *A*, GATA3 and JunB protein expression in developing Th2 cells. Naive CD4<sup>+</sup> T cells from BALB/c mice were stimulated with anti-TCR $\beta$  mAb in the presence of IL-4 and anti-IL-12 mAb for 5 days, and total nuclear extracts were analyzed by immunoblotting with anti-GATA3 mAb, anti-JunB mAb, or anti-tubulin- $\alpha$  mAb. Three independent experiments were performed; representative results are shown. Arbitrary densitometric units normalized to tubulin- $\alpha$  are shown under each band. *B*, GATA3 mRNA expression in young and aging developing Th2 cells. Th2 cells prepared as in *A* were subjected to quantitative RT-PCR analysis. *C*, Naive CD4<sup>+</sup> T cells from BALB/c mice were stimulated with anti-TCR $\beta$  mAb in the presence of IL-4 and anti-IL-12 mAb for 2 days and then infected with a mock or GATA3-containing retrovirus vector. Th1/Th2 cell differentiation was assessed on day 5.

*Decreased OVA-induced eosinophilic infiltration in BAL fluid and airway inflammation in aging mice*

Next, we examined the effect of aging on Th2-dependent immune responses in vivo. Young and aging BALB/c mice were immunized twice with OVA-alum, and 2 wk later, exposed to inhaled OVA as described in *Materials and Methods*. BAL fluid was harvested and examined for infiltrating leukocytes (Fig. 8, *A* and *B*). Eosinophils, lymphocytes, neutrophils, and macrophages were determined based on morphological criteria, and the absolute numbers and percentages of each cell type were determined. A substantial decrease in the absolute numbers (Fig. 8*A*) and percentages

**FIGURE 7.** Histone modification of the Th2-cytokine locus in developing Th2 cells from aging mice. *A*, Acetylation and methylation status of histones associated with the Th2 cytokine gene locus. Freshly prepared naive splenic CD4<sup>+</sup> T cells were stimulated under Th1 or Th2 conditions for 5 days. The acetylation status and methylation status of histone H3 in nucleosomes associated with the indicated regions was assessed by ChIP assay. An anti-acetylated histone H3 (K9 and K14) Ab and an anti-histone H3 di-methyl K4 antiserum were used. *B*, The relative intensity of histone hyperacetylation (Ac-H3/input) in each group is shown in *A*. *C*, The relative intensity of histone dimethylation (diMe-H3/input) in each group is shown in *A*. Representative results of three independent experiments are shown.

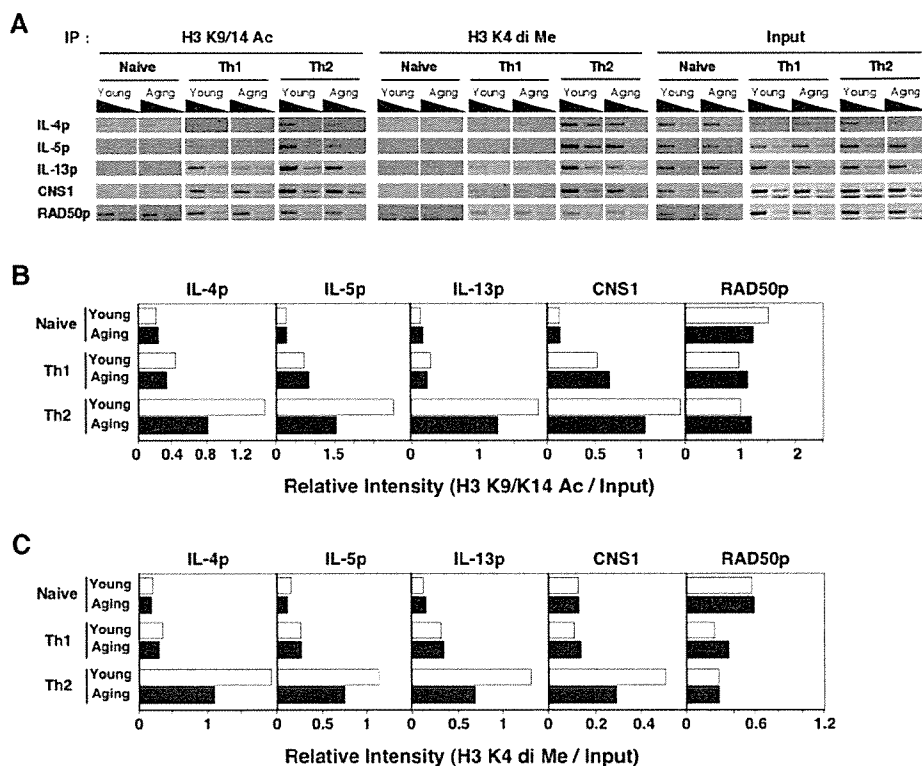


(Fig. 8B) of eosinophils was observed in aging mice. The infiltration of macrophages was increased in aging mice, and the number of total infiltrating cells was decreased in aging mice. These results indicate that OVA-induced eosinophilic infiltration in the BAL fluid is decreased in aging mice.

Concurrently, histological changes in the lungs of young and aging mice were evaluated by HE staining (Fig. 8C). The absolute numbers and percentages of each cell type are shown (Fig. 8, D and E). The numbers of total infiltrating cells were indistinguishable between young and aging mice, although a slight decrease in the absolute number, and a slight, but significant, decrease in the percentage of eosinophils were observed. No apparent difference in the numbers of lymphocytes, neutrophils or macrophages was observed.

## Discussion

In the present study, we used young adult (4–6 wk old) and aging (8–12 mo old) mice, to demonstrate that the levels of Th2 cell differentiation and Th2-dependent allergic airway inflammation are attenuated in aging mice. In addition, we found several molecular defects in aging mouse CD4<sup>+</sup> T cells, i.e., limited activation of the ERK/MAPK cascade, decreased expression of GATA3 and impaired chromatin remodeling of the Th2 cytokine gene locus. Because 8- to 12-wk-old mice can be considered to be in the early stages of aging, the processes affected would be the most sensitive among various age-related alterations in T cells.

Impaired Th2 cell differentiation in aging mouse CD4<sup>+</sup> T cell cultures was not restored by the addition of excess amounts of exogenous IL-4 (10 U/ml; Fig. 2, middle panel). In addition, our in vitro cultures contained sufficient amounts of exogenous IL-2 (30 U/ml). The production of all Th2 cytokines (IL-4, IL-5, and IL-13) was decreased in aging mouse CD4<sup>+</sup> T cells (Fig. 3). Thus, the defect in Th2 cell differentiation appears to be due to intrinsic alterations and not simply a secondary consequence of the imbalance

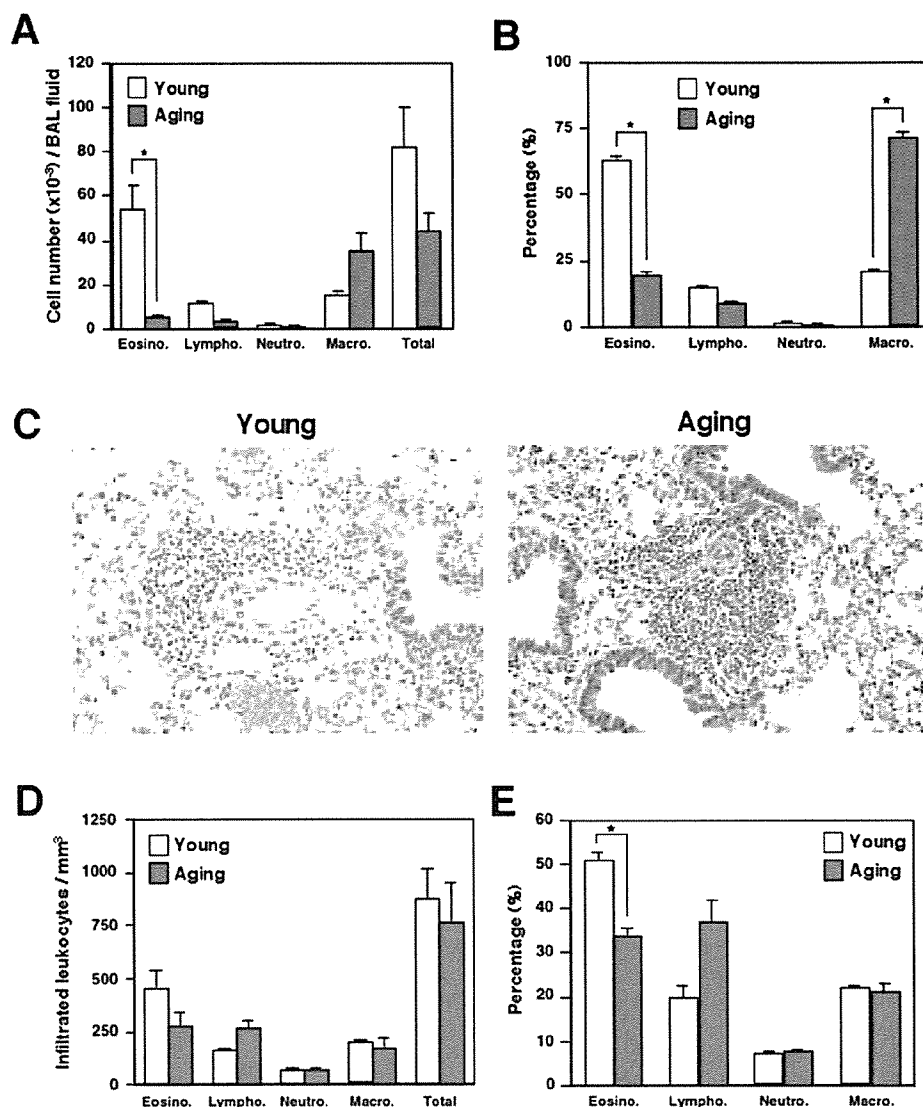
in the production of IL-2, IL-4, or IFN- $\gamma$  by aging mouse CD4<sup>+</sup> T cells in culture. Our observations are consistent with the results reported by H. al-Rayes et al. (52) that IL-4 production is diminished in aged human PBL.

In our previous reports, we showed that Th2 cell differentiation and Th2-dependent airway inflammation are highly dependent on the TCR-mediated activation of the Ras-ERK MAPK cascade (6, 48). In the present study, we detected significantly reduced activation of the Ras/MAPK cascade in aging mouse CD4<sup>+</sup> T cells (Fig. 5D). Thus, the impaired Th2 cell differentiation in old mice appears to be due to the decreased TCR-mediated activation of the Ras/MAPK signaling pathway.

As for Th1 cell differentiation, we observed no detectable decrease in IL-12-induced Th1 cell generation in vitro (Fig. 2, right panels), suggesting that the efficiency in Th1 cell differentiation is less affected by aging. We detected significant numbers of IFN- $\gamma$  producing cells in aging naive CD4<sup>+</sup> T cell cultures when exogenous IL-4 was not included in the culture (Fig. 2, left panels). In addition, we detected increased production of IFN- $\gamma$  by ELISA (Fig. 3). These results suggest that some shift from Th2 to Th1 cell differentiation occurs in aging mouse CD4<sup>+</sup> T cell cultures. We previously reported a dramatic shift from Th2 to Th1 cell differentiation in dominant negative Ras Tg mice (6). Therefore, these results also support the notion that the impaired Th2 cell differentiation in aging mice is due to the decreased TCR-mediated activation of the Ras/MAPK signaling pathway.

The expression levels of the GATA3 protein are critical for chromatin remodeling (46) and the maintenance of remodeled chromatin at the Th2 cytokine gene locus (14). In addition, we have recently demonstrated that the activation of the Ras-ERK MAPK cascade controls the stability of the GATA3 protein through the inhibition of ubiquitin-dependent degradation (16). The results presented in this report suggest that GATA3-dependent

**FIGURE 8.** OVA-induced eosinophilic infiltration in BAL fluid and airway inflammation in old mice. The absolute cell number (A) and percentage (B) of eosinophils (Eosino.), lymphocytes (Lympho.), neutrophils (Neutro.), and macrophages (Macro.) in BAL fluid are shown with SDs. Three young (6 wk-old) and three aging (9 mo-old) BALB/c mice were used in this experiment. Data include absolute cell number, percentage of cells, total cell number per milliliter, and the volume of BAL fluid recovered. \*,  $p < 0.01$  and other  $p$  values  $>0.05$  by Student's  $t$  test. C, OVA immunization and inhalation of OVA aerosol were done as in A. The lungs were fixed and stained with H&E,  $\times 200$ . Sections shown are representative of 10 lung sections/mouse from three mice in each group. The cell number (D) and percentage (E) of infiltrated eosinophils (Eosino.), lymphocytes (Lympho.), neutrophils (Neutro.), and macrophages (Macro.) in the perivascular and peribronchiolar regions are shown with SDs. Three young (6 wk old) and three aging (9 mo old) BALB/c mice were used in this experiment. \*,  $p < 0.01$  and other  $p$  values  $>0.05$  by Student's  $t$  test.



chromatin remodeling of the Th2 cytokine gene locus is significantly reduced in aging mouse CD4<sup>+</sup> T cells (Fig. 7). The expression levels of JunB (Fig. 6A) and the activation of NF- $\kappa$ B were comparable between young and aging mouse CD4<sup>+</sup> T cells (A. Hasegawa and T. Nakayama, unpublished observation). From these results, we conclude that the impaired chromatin remodeling of the Th2 cytokine gene locus in aging mice is due, at least in part, to the decreased expression of the GATA3 protein in developing Th2 cells.

Although it remains unclear why the activation of the Ras-ERK MAPK cascade is affected selectively during aging, this pathway may determine the characters of various T cell responses. In anergic CD4 T cells impaired activation of the Ras-ERK MAPK cascade has been reported (53, 54).

How allergic inflammation, such as allergic asthma is modulated by aging has not been reported. We show in the present study that the severity of Th2-dependent allergic airway inflammation is decreased in aging mice (Fig. 7). This appears to be due to the decreased Th2 cell differentiation in aging mice. Although there is as yet no clear evidence in humans, the data would suggest that the first onset of allergic asthma should occur less frequently in aged human beings. The confirmation of this hypothesis must await a comprehensive investigation in humans.

In summary, this study provides the first evidence that a chromatin-remodeling event in T cells, i.e., chromatin remodeling of the Th2 cytokine gene locus in developing Th2 cells, is compromised during aging. Moreover, we demonstrate attenuated Th2-dependent allergic airway inflammation in aging mice, which may reflect the nature of allergic diseases in aged humans.

**Acknowledgments**

We thank Kaoru Sugaya for excellent technical assistance.

**Disclosures**

The authors have no financial conflict of interest.

**References**

- Mosmann, T. R., and R. L. Coffman. 1989. Th1 and Th2 cells: different patterns of lymphokine secretion lead to different functional properties. *Annu. Rev. Immunol.* 7: 145-173.
- Abbas, A. K., K. M. Murphy, and A. Sher. 1996. Functional diversity of helper T lymphocytes. *Nature* 383: 787-793.
- Constant, S. L., and K. Bottomly. 1997. Induction of Th1 and Th2 CD4<sup>+</sup> T cell responses: the alternative approaches. *Annu. Rev. Immunol.* 15: 297-322.
- O'Garra, A. 1998. Cytokines induce the development of functionally heterogeneous T helper cell subsets. *Immunity* 8: 275-283.
- Yamashita, M., K. Hashimoto, M. Kinura, M. Kubo, T. Tada, and T. Nakayama. 1998. Requirement for p56<sup>lck</sup> tyrosine kinase activation in Th subset differentiation. *Int. Immunol.* 10: 577-591.

6. Yamashita, M., M. Kimura, M. Kubo, C. Shimizu, T. Tada, R. M. Perlmutter, and T. Nakayama. 1999. T cell antigen receptor-mediated activation of the Ras/mitogen-activated protein kinase pathway controls interleukin 4 receptor function and type-2 helper T cell differentiation. *Proc. Natl. Acad. Sci. USA* 96: 1024–1029.
7. Yamashita, M., M. Katsumata, M. Iwashima, M. Kimura, C. Shimizu, T. Kamata, T. Shin, N. Seki, S. Suzuki, M. Taniguchi, and T. Nakayama. 2000. T cell receptor-induced calcineurin activation regulates T helper type 2 cell development by modifying the interleukin 4 receptor signaling complex. *J. Exp. Med.* 191: 1869–1879.
8. Grogan, J. L., and R. M. Locksley. 2002. T helper cell differentiation: on again, off again. *Curr. Opin. Immunol.* 14: 366–372.
9. Murphy, K. M., and S. L. Reiner. 2002. The lineage decisions of helper T cells. *Nat. Rev. Immunol.* 2: 933–944.
10. Zhang, D. H., L. Cohn, P. Ray, K. Bottomly, and A. Ray. 1997. Transcription factor GATA-3 is differentially expressed in murine Th1 and Th2 cells and controls Th2-specific expression of the interleukin-5 gene. *J. Biol. Chem.* 272: 21597–21603.
11. Zheng, W., and R. A. Flavell. 1997. The transcription factor GATA-3 is necessary and sufficient for Th2 cytokine gene expression in CD4 T cells. *Cell* 89: 587–596.
12. Ouyang, W., S. H. Ranganath, K. Weindel, D. Bhattacharya, T. L. Murphy, W. C. Sha, and K. M. Murphy. 1998. Inhibition of Th1 development mediated by GATA-3 through an IL-4-independent mechanism. *Immunity* 9: 745–755.
13. Lee, H. J., N. Takemoto, H. Kurata, Y. Kamogawa, S. Miyatake, A. O'Garra, and N. Arai. 2000. GATA-3 induces T helper cell type 2 (Th2) cytokine expression and chromatin remodeling in committed Th1 cells. *J. Exp. Med.* 192: 105–115.
14. Yamashita, M., M. Ukai-Tadenuma, T. Miyamoto, K. Sugaya, H. Hosokawa, A. Hasegawa, M. Kimura, M. Taniguchi, J. DeGregori, and T. Nakayama. 2004. Essential role of GATA3 for the maintenance of type 2 helper T (Th2) cytokine production and chromatin remodeling at the Th2 cytokine gene loci. *J. Biol. Chem.* 279: 26983–26990.
15. Pai, S. Y., M. L. Truitt, and I. C. Ho. 2004. GATA-3 deficiency abrogates the development and maintenance of T helper type 2 cells. *Proc. Natl. Acad. Sci. USA* 101: 1993–1998.
16. Yamashita, M., R. Shinnakasu, H. Asou, M. Kimura, A. Hasegawa, K. Hashimoto, N. Hatano, M. Ogata, and T. Nakayama. 2005. Ras-ERK MAPK cascade regulates GATA3 stability and Th2 differentiation through ubiquitin-proteasome pathway. *J. Biol. Chem.* 280: 29409–29419.
17. Miller, R. A. 1996. The aging immune system: primer and prospectus. *Science* 273: 70–74.
18. Globerson, A., and R. B. Effros. 2000. Ageing of lymphocytes and lymphocytes in the aged. *Immunol. Today* 21: 515–521.
19. Webster, R. G. 2000. Immunity to influenza in the elderly. *Vaccine* 18: 1686–1689.
20. Miller, R. A. 2000. Effect of aging on T lymphocyte activation. *Vaccine* 18: 1654–1660.
21. Chakravarti, B., and G. N. Abraham. 1999. Aging and T cell-mediated immunity. *Mech. Ageing Dev.* 108: 183–206.
22. Haynes, L., S. M. Eaton, E. M. Burns, T. D. Randall, and S. L. Swain. 2005. Newly generated CD4 T cells in aged animals do not exhibit age-related defects in response to antigen. *J. Exp. Med.* 201: 845–851.
23. Linton, P. J., L. Haynes, L. Tsui, X. Zhang, and S. Swain. 1997. From naive to effector: alterations with aging. *Immunol. Rev.* 160: 9–18.
24. Gillis, S., R. Kozak, M. Durante, and M. E. Weksler. 1981. Immunological studies of aging: decreased production of and response to T cell growth factor by lymphocytes from aged humans. *J. Clin. Invest.* 67: 937–942.
25. Engwerda, C. R., B. S. Handwerker, and B. S. Fox. 1996. An age-related decrease in rescue from T cell death following costimulation mediated by CD28. *Cell. Immunol.* 170: 141–148.
26. Ginaldi, L., M. De Martinis, A. D'Ostilio, L. Marini, M. F. Loreto, M. P. Corsi, and D. Quaglino. 2000. Cell proliferation and apoptosis in the immune system in the elderly. *Immunol. Res.* 21: 31–38.
27. Li, M., R. Walter, C. Torres, and F. Sierra. 2000. Impaired signal transduction in mitogen activated rat splenic lymphocytes during aging. *Mech. Ageing Dev.* 113: 85–99.
28. Damjanovich, S., R. Gaspar, Jr., L. Bene, A. Jenei, and L. Matyus. 2003. Signal transduction in T lymphocytes and aging. *Exp. Gerontol.* 38: 231–236.
29. Garcia, G. G., and R. A. Miller. 1998. Increased Zap-70 association with CD3 $\zeta$  in CD4 T cells from old mice. *Cell. Immunol.* 190: 91–100.
30. Miller, R. A. 1997. Age-related changes in T cell surface markers: a longitudinal analysis in genetically heterogeneous mice. *Mech. Ageing Dev.* 96: 181–196.
31. Cossarizza, A., C. Ortolani, R. Paganelli, D. Barbieri, D. Monti, P. Sansoni, U. Fagiolo, G. Castellani, F. Bersani, M. Londei, and C. Franceschi. 1996. CD45 isoforms expression on CD4<sup>+</sup> and CD8<sup>+</sup> T cells throughout life, from newborns to centenarians: implications for T cell memory. *Mech. Ageing Dev.* 86: 173–195.
32. Bandres, E., J. Merino, B. Vazquez, S. Inoges, C. Moreno, M. L. Subira, and A. Sanchez-Ibarra. 2000. The increase of IFN- $\gamma$  production through aging correlates with the expanded CD8<sup>+</sup>CD28<sup>-</sup>CD57<sup>+</sup> subpopulation. *Clin. Immunol.* 96: 230–235.
33. Sakata-Kaneko, S., Y. Wakatsuki, Y. Matsunaga, T. Usui, and T. Kita. 2000. Altered Th1/Th2 commitment in human CD4<sup>+</sup> T cells with ageing. *Clin. Exp. Immunol.* 120: 267–273.
34. Poynter, M. E., and R. A. Daynes. 1999. Age-associated alterations in splenic iNOS regulation: influence of constitutively expressed IFN- $\gamma$  and correction following supplementation with PPAR $\alpha$  activators or vitamin E. *Cell. Immunol.* 195: 127–136.
35. Karanfilov, C. I., B. Liu, C. C. Fox, R. R. Lakshmanan, and R. L. Whisler. 1999. Age-related defects in Th1 and Th2 cytokine production by human T cells can be dissociated from altered frequencies of CD45RA<sup>+</sup> and CD45RO<sup>+</sup> T cell subsets. *Mech. Ageing Dev.* 109: 97–112.
36. Mbowu, I. N., C. L. Acuna, K. C. Walz, R. L. Atmar, S. B. Greenberg, and R. B. Couch. 1997. Cytokines and impaired CD8<sup>+</sup> CTL activity among elderly persons and the enhancing effect of IL-12. *Mech. Ageing Dev.* 94: 25–39.
37. Rink, L., I. Cakman, and H. Kirchner. 1998. Altered cytokine production in the elderly. *Mech. Ageing Dev.* 102: 199–209.
38. Ernst, D. N., M. V. Hobbs, B. E. Torbett, A. L. Glasebrook, M. A. Rehse, K. Bottomly, K. Hayakawa, R. R. Hardy, and W. O. Weigle. 1990. Differences in the expression profiles of CD45RB, Pgp-1, and 3G11 membrane antigens and in the patterns of lymphokine secretion by splenic CD4<sup>+</sup> T cells from young and aged mice. *J. Immunol.* 145: 1295–1302.
39. Kubo, M., and B. Cincader. 1990. Polymorphism of age-related changes in interleukin (IL) production: differential changes of T helper subpopulations, synthesizing IL 2, IL 3 and IL 4. *Eur. J. Immunol.* 20: 1289–1296.
40. Murphy, K. M., A. B. Heimberger, and D. Y. Loh. 1990. Induction by antigen of intrathymic apoptosis of CD4<sup>+</sup>CD8<sup>+</sup>TCR<sup>low</sup> thymocytes in vivo. *Science* 250: 1720–1723.
41. Nakayama, T., C. H. June, T. I. Munitz, M. Sheard, S. A. McCarthy, S. O. Sharrow, L. E. Samelson, and A. Singer. 1990. Inhibition of T cell receptor expression and function in immature CD4<sup>+</sup>CD8<sup>+</sup> cells by CD4. *Science* 249: 1558–1561.
42. Kimura, M., Y. Koseki, M. Yamashita, N. Watanabe, C. Shimizu, T. Katsumoto, T. Kitamura, M. Taniguchi, H. Koseki, and T. Nakayama. 2001. Regulation of Th2 cell differentiation by mel-18, a mammalian polycomb group gene. *Immunity* 15: 275–287.
43. Inami, M., M. Yamashita, Y. Tenda, A. Hasegawa, M. Kimura, K. Hashimoto, N. Seki, M. Taniguchi, and T. Nakayama. 2004. CD28 costimulation controls histone hyperacetylation of the interleukin 5 gene locus in developing Th2 cells. *J. Biol. Chem.* 279: 23123–23133.
44. Kimura, M. Y., H. Hosokawa, M. Yamashita, A. Hasegawa, C. Iwamura, H. Watarai, M. Taniguchi, T. Takagi, S. Ishii, and T. Nakayama. 2005. Regulation of T helper type 2 cell differentiation by murine Schnurri-2. *J. Exp. Med.* 201: 397–408.
45. Omori, M., M. Yamashita, M. Inami, M. Ukai-Tadenuma, M. Kimura, Y. Nigo, H. Hosokawa, A. Hasegawa, M. Taniguchi, and T. Nakayama. 2003. CD8 T cell-specific down-regulation of histone hyperacetylation and gene activation of the IL-4 gene locus by ROG, repressor of GATA. *Immunity* 19: 281–294.
46. Yamashita, M., M. Ukai-Tadenuma, M. Kimura, M. Omori, M. Inami, M. Taniguchi, and T. Nakayama. 2002. Identification of a conserved GATA3 response element upstream proximal from the interleukin-13 gene locus. *J. Biol. Chem.* 277: 42399–42408.
47. Yamashita, M., R. Shinnakasu, Y. Nigo, M. Kimura, A. Hasegawa, M. Taniguchi, and T. Nakayama. 2004. Interleukin (IL)-4-independent maintenance of histone modification of the IL-4 gene loci in memory Th2 cells. *J. Biol. Chem.* 279: 39454–39464.
48. Shibata, Y., T. Kamata, M. Kimura, M. Yamashita, C. R. Wang, K. Murata, M. Miyazaki, M. Taniguchi, N. Watanabe, and T. Nakayama. 2002. Ras activation in T cells determines the development of antigen-induced airway hyperresponsiveness and eosinophilic inflammation. *J. Immunol.* 169: 2134–2140.
49. Hansen, G., G. Berry, R. H. DeKruyff, and D. T. Umetsu. 1999. Allergen-specific Th1 cells fail to counterbalance Th2 cell-induced airway hyperreactivity but cause severe airway inflammation. *J. Clin. Invest.* 103: 175–183.
50. Foster, P. S., S. P. Hogan, A. J. Ramsay, K. I. Matthaei, and I. G. Young. 1996. Interleukin 5 deficiency abolishes eosinophilia, airways hyperreactivity, and lung damage in a mouse asthma model. *J. Exp. Med.* 183: 195–201.
51. Kamata, T., M. Yamashita, M. Kimura, K. Murata, M. Inami, C. Shimizu, K. Sugaya, C. R. Wang, M. Taniguchi, and T. Nakayama. 2003. *src* homology 2 domain-containing tyrosine phosphatase SHP-1 controls the development of allergic airway inflammation. *J. Clin. Invest.* 111: 109–119.
52. al-Rayes, H., W. Pachas, N. Mirza, D. J. Ahern, R. S. Geha, and D. Vercelli. 1992. IgE regulation and lymphokine patterns in aging humans. *J. Allergy Clin. Immunol.* 90: 630–636.
53. Li, W., C. D. Whaley, A. Mondino, and D. L. Mueller. 1996. Blocked signal transduction to the ERK and JNK protein kinases in anergic CD4<sup>+</sup> T cells. *Science* 271: 1272–1276.
54. Fields, P. E., T. F. Gajewski, and F. W. Fitch. 1996. Blocked Ras activation in anergic CD4<sup>+</sup> T cells. *Science* 271: 1276–1278.

## Lentivirus vectors expressing short hairpin RNAs against the *U3*-overlapping region of HIV *nef* inhibit HIV replication and infectivity in primary macrophages

Takuya Yamamoto, Hiroyuki Miyoshi, Norio Yamamoto, Naoki Yamamoto, Jun-ichiro Inoue, and Yasuko Tsunetsugu-Yokota

Although successful attempts to inhibit HIV-1 replication in T cells using RNAi have been reported, the effect of HIV-specific RNAi on macrophages is not well known. Macrophages are key targets for anti-HIV-1 therapy because they are able to survive long after the initial infection with HIV and can spread the virus to T cells. In this study, we identified a putative RNAi target of HIV, consisting of the portion of the *nef* gene overlapping the U3 region (Nef366), and generated a lenti-

virus-based short hairpin RNA (shRNA) expression vector (Lenti shNef366). We show that Lenti shNef366 inhibits (1) HIV-1 replication in a monocytic cell line and in primary monocyte-derived macrophages (MDMs), (2) reactivation of latent HIV-1 infection, and (3) the production of secondary HIV-1 from MDMs harboring a genomic copy of Nef366. Moreover, we found that the up-regulated production of macrophage inflammatory protein 1 $\beta$  (MIP-1 $\beta$ ), but not MIP-1 $\alpha$ , in MDMs by Nef

expression was considerably suppressed by Lenti shNef366, which suggests that HIV-1 dissemination to T cells through its interaction with HIV-1-infected MDMs can also be controlled by Lenti shNef366. Thus, lentivirus-mediated shRNA expression targeting the U3-overlapping region of HIV *nef* represents a feasible approach to genetic vaccine therapy for HIV-1. (Blood. 2006;108:3305-3312)

© 2006 by The American Society of Hematology

### Introduction

HIV Nef, which is uniquely conserved among HIV-1, HIV-2, and SIV, is essential for viral replication *in vivo*.<sup>1</sup> Nef is located at the 3' end of the viral genome, partially overlapping the 3' long terminal repeat (LTR). The *nef* gene is one of the earliest expressed genes during HIV-1 replication and is transcribed at particularly high levels, often accounting for up to 80% of HIV-1-specific RNA in the early stages of viral replication. The Nef protein is multifunctional, having been shown to be involved in the down-regulation of CD4 receptor molecules, cell apoptosis, and signal transduction.<sup>2-6</sup> From studies of HIV-infected individuals, accumulating evidence indicates that Nef plays an important, albeit currently not clearly understood, role in the pathogenesis of AIDS.<sup>1,2,6,7</sup>

Recent investigations have shown that Nef has evolved macrophage-specific functions, such as the recruitment of T cells to sites of infection.<sup>8</sup> Macrophages expressing Nef secrete a high level of macrophage inflammatory protein 1 $\alpha$  (MIP-1 $\alpha$ ) and MIP-1 $\beta$ , thus recruiting peripheral T cells to lymph nodes. More recently it was shown that Nef regulates the release of paracrine factors from macrophages<sup>9</sup>; at least 2 proteins have been identified, which enhance lymphocyte susceptibility to HIV-1 infection in the absence of cell-cycle progression. These

results provide ample evidence that Nef functions as a virulence factor that contributes to the manifestation of the clinical symptoms of immunodeficiency. Thus, any therapeutic intervention aimed at either completely blocking or at least partially reducing the expression of *nef* during HIV infection would likely enhance the ability of the immune system to fight HIV infection.

Sequence-specific degradation of viral mRNA by the process of RNAi is a mechanism for selectively inhibiting the synthesis of viral proteins that are critical for HIV-1 replication. RNAi therapy is based on an existing mechanism of gene regulation that is ubiquitous in plants and animals, in which targeted mRNAs are degraded in a sequence-specific manner.<sup>10</sup> Quite recently, several groups reported the use of RNAi to successfully inhibit HIV-1 replication.<sup>11-15</sup>

To study the effect of stable expression of short hairpin RNA (shRNA) against the U3-overlapping region of HIV-1 *nef* on virus replication and Nef-mediated cytokine regulation in primary macrophages, we established a lentivirus vector system expressing HIV-specific shRNAs. We show that HIV replication in primary macrophages was considerably suppressed following transfection of shRNAs targeting the U3-overlapping region of genomic HIV *nef*. Moreover, RNAi was able to control CC-chemokine

From the Department of Immunology, National Institute of Infectious Diseases, Toyama, Shinjuku-ku, Tokyo; Subteam for Manipulation of Cell Fate, BioResource Center, RIKEN Tsukuba Institute, Tsukuba; Department of Molecular Virology, Bio-Response, Tokyo Medical and Dental University, Bunkyo-ku, Tokyo; AIDS Research Center, National Institute of Infectious Diseases, Shinjuku, Tokyo; and Division of Cellular and Molecular Biology, Department of Cancer Biology, Institute of Medical Science, University of Tokyo, Shirokane-dai, Minato-ku, Tokyo, Japan.

Submitted April 6, 2006; accepted June 29, 2006. Prepublished online as *Blood* First Edition Paper, July 20, 2006; DOI 10.1182/blood-2006-04-014829.

Supported by a grant from the Ministry of Health, Labor, and Welfare of Japan and from the Japan Health Sciences Foundation.

The authors declare no competing financial interests.

T.Y. and Y.T.-Y. performed laboratory experiments, data management, and the biostatistical analysis; T.Y., Naoki Y., J.-i.I., and Y.T.-Y. were responsible for the general design of the study; H.M. and Norio Y. were responsible for the design of the specific parts on lentivirus vectors and quantitative PCR analysis, respectively; T.Y., Y.T.-Y., and J.-i.I. were involved in the interpretation of the results and general outline of the paper; and T.Y. and Y.T.-Y. wrote the article.

**Reprints:** Yasuko Tsunetsugu-Yokota, Department of Immunology, National Institute of Infectious Diseases, Toyama 1-23-1, Shinjuku-ku, Tokyo 162-8640, Japan; e-mail: yyokota@nih.go.jp.

The publication costs of this article were defrayed in part by page charge payment. Therefore, and solely to indicate this fact, this article is hereby marked "advertisement" in accordance with 18 USC section 1734.

© 2006 by The American Society of Hematology

production associated with Nef expression in HIV-1-infected macrophages. Thus, lentivirus-vector-based RNAi of the U3-overlapping region of HIV-1 *nef* might have potential usefulness as a genetic vaccine against HIV-1 infection.

## Materials and methods

### Construction of plasmids

To express gene-specific shRNAs under the human U6-RNA promoter, sense and antisense oligonucleotides 47 bp in length were ligated into pENTR/U6 (Invitrogen, Carlsbad, CA). The sequences of the oligonucleotides were as follows: *lacZ*, sense oligonucleotide, 5'-caccgctacacaatcagcagcttcgaaaaatcgctgattgtgtag-3', and antisense oligonucleotide, 5'-aaaactacacaatcagcagctttcgaatcgcgattgtgtagc-3'; *Nef366* (nucleotides 366-385 of the HIV-1<sub>NL432</sub> *nef* ORF overlapping the 3' LTR), sense oligonucleotide, 5'-caccgattggcagaactacacacagaagagtgtagtttgcacaac-3', and antisense oligonucleotide, 5'-aaaagattggcagaactacacactctcttggtgtgtagtttgcacaac-3'. The resulting entry vectors were termed pENTR/shLacZ and pENTR/shNef366, respectively.

A Gateway-compatible (Invitrogen) HIV-1-based vector, pCS-RfA, containing elongation factor 1 $\alpha$  promoter (EF-1 $\alpha$ )-driven green fluorescent protein (EGFP) (pCS-RfA-EG),<sup>16</sup> was used to construct the lentivirus vectors, pCS-EG/shLacZ and pCS-EG/shNef366, according to the manufacturer's instructions (Invitrogen).

### Cell culture and transfection

The human cell line 293T and human monocytic cell lines U937 and U1<sup>17</sup> were maintained in Dulbecco modified Eagle medium (DMEM) and RPMI 1640 medium (Gibco, Grand Island, NY), respectively, supplemented with 10% heat-inactivated fetal calf serum (FCS), penicillin (100  $\mu$ g/mL), and streptomycin (100  $\mu$ g/mL). To establish CCR5<sup>+</sup> CEMx174 cells expressing EGFP driven by HIV-LTR, CEMx174 cells were transfected with pEF-BOSbst-HuCCR5 and pHIV-1 LTR-EGFPpuro (kind gifts from M. Tatsumi, National Institute of Infectious Diseases, Tokyo, Japan) and CEMx174 CCR5/LTR-EGFP cells were established.

HeLa-CD4 cells (obtained from the National Institutes of Health AIDS Reagent Program) were transfected with pEF-Nef bst. and Nef-expressing HeLa-CD4 cells were established (HeLa-CD4-Nef).

### RNAi target site selection

A Web-based program for designing siRNA targets (Promega, Madison, WI), BLOCK-iT RNAi Target Designer (Invitrogen), and the National Center for Biotechnology Information Web site were used for the selection of siRNA and shRNA sequences, and for BLAST searches. Stealth siRNAs were synthesized (Figure 1) and HeLa-CD4-Nef cells were transfected with 2.5  $\mu$ L stealth siRNA complexed to 2.5  $\mu$ L Lipofectamine 2000 (Invitrogen) according to the manufacturer's instructions. Total RNA was extracted and analyzed by quantitative reverse transcription-polymerase chain reaction (qRT-PCR) using specific LUX primers (Invitrogen) and the SuperScript III Platinum One-Step Quantitative RT-PCR system (Invitrogen). The sequences of the qRT-PCR primers were as follows: *nef* forward, labeled at its 3' terminus with a reporter fluorophore 6-carboxyfluorescein (FAM), 5'-cageagagtgtagtgtagcctgcFAMg-3'; *nef* reverse, 5'-tggctcagctcgtctcattctt-3'; *ef-1 $\alpha$*  forward labeled at its 3' terminus with a reporter fluorophore 6-carboxy-4', 5'-dichloro-2', 7'-dimethoxyfluorescein (JOE), 5'-gaaccacaagtgcatacatcctggJOEtc-3'; *ef-1 $\alpha$*  reverse, 5'-agcgtggtccactggcatt-3'. The reactions were performed using an Mx3000P (Stratagene, La Jolla, CA).

For Western blot analysis, cell lysates were prepared, subjected to 12.5% sodium dodecyl sulfate-polyacrylamide gel electrophoresis (SDS-PAGE), and immunoblotted with anti-Nef monoclonal antibody (mAb: F3, a kind gift from Dr Y. Fuji, Graduate School of Pharmaceutical Science, Nagoya City University, Nagoya, Japan). The blot was reacted with biotinylated goat anti-mouse IgG antibody (Jackson ImmunoResearch, West Grove, PA), then with streptavidin-POD (Roche, Indianapolis, IN).

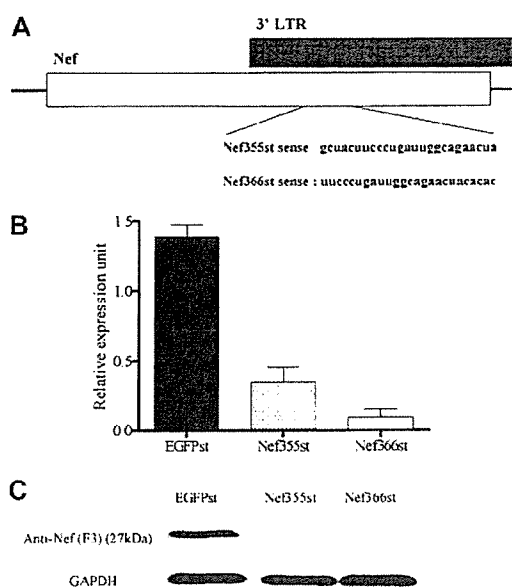


**Figure 1.** siRNA target sequences in *nef*. (A) Targets of siRNAs against the U3-overlapping region of HIV-1<sub>NL432</sub> Nef and their sequences. Nef-expressing HeLa CD4 cells were transfected either with 2.5  $\mu$ M *egfp* siRNAs (control: EGFPst) or *nef* siRNAs (Nef355st or Nef366st). At 48 hours after transfection, these cells were lysed to obtain total RNA and protein. (B) Total RNA was extracted and analyzed by qRT-PCR. The level of *nef* mRNA expression was normalized with that of elongation factor 1 $\alpha$  (EF-1 $\alpha$ ) mRNA expression (*nef*/EF-1 $\alpha$ ). The data represent the expression level of *nef* mRNA relative to that of the control as 100%. The data represent the average  $\pm$  SD of 3 independent experiments. (C) The cell lysates were subjected to 12.5% SDS-PAGE and immunoblotted with anti-Nef mAb.

Proteins were visualized by the SuperSignal Western Dura Extended Duration Substrate (Pierce, Rockford, IL) using an LAS3000 analyzer (Fuji Film, Tokyo, Japan).

### Preparation of lentivirus vector

The lentivirus shRNA expression vectors were produced by transient transfection of 293T cells with a self-inactivating (SIN) vector construct, VSV-G- and Rev-expressing plasmid pCMV-VSV-G-RSV-Rev, and the packaging construct pCAG-HIVgp using the calcium phosphate precipitation method.<sup>16</sup> The lentiviral vector was concentrated by ultracentrifugation and the final solution was assayed for p24 antigen by an in-house enzyme-linked immunosorbent assay (ELISA).<sup>18</sup> The infectivity was determined by using 293T cells based on the EGFP expression.

### Preparation of HIV-1 virus stocks

To prepare HIV-1, COS-7 cells were transfected with either pNL432, pNF462 (a kind gift from A. Adachi, Tokushima University, Tokushima, Japan), or pNF462dNef, in which the *nef* gene was deleted by digestion with *Xho*I and *Kpn*I, as described previously.<sup>18</sup>

### Primary MDM culture

From peripheral blood mononuclear cells (PBMCs) of healthy, HIV-1<sup>-</sup> donors, CD14<sup>+</sup> monocytes were enriched using a magnetic-activated cell sorter (MACS; Miltenyi Biotec, Cologne, Germany) as described.<sup>18</sup> Monocytes were cultivated in RPMI 1640 medium supplemented with 10% FCS, 5% human AB plasma, and 10 ng/mL macrophage colony-stimulating factor (M-CSF) for 1 week to allow differentiation into monocyte-derived macrophages (MDMs).

### Kinetics of virus production in stable shRNA-expressing U937 cells

Stable shRNA-expressing cells were infected with HIV-1<sub>NL432</sub> for 2 hours, then cells were washed 5 times. Culture supernatants were harvested at 3- or

4-day intervals and viral production was monitored by HIV-1 p24 Gag antigen ELISA kit (RETRO-TEC; ZepetoMetrix, Buffalo, NY).

#### Real-time RT-PCR (qRT-PCR) analysis of HIV-1 infection

HIV-1-infected cells were collected and total DNA was prepared 3, 8 and 12 hours after infection. For the detection and quantification of individual forms of HIV-1 DNA, oligonucleotide primer and probe sequences were designed specifically for the TaqMan assay as described elsewhere.<sup>19</sup> All probes (Biosearch Technologies, Novato, CA) were 5'-labeled with the fluorophore FAM as the reporter dye, and 3'-labeled with Black Hole Quencher-1 (BHQ-1) as the quencher dye. The qRT-PCR analysis was performed on an Mx3000P (Stratagene) and the amount of HIV-1-specific DNA per cell was normalized to  $\beta$ -globin gene.

#### Kinetics of virus production in MDMs and reporter analysis

MDMs ( $2 \times 10^5$ /well) were cultured in 48-well tissue-culture plates and infected either with wild-type HIV-1<sub>NF462</sub> or HIV-1<sub>NF462ΔNef</sub>. MDMs were infected with lentivirus at a multiplicity of infection (MOI) of 2 or 10 and washed extensively. The next day, cells were exposed to HIV-1 (5 ng/well) for 2 hours. Cell supernatants were harvested at 3- or 4-day intervals, and viral production was monitored by p24 antigen ELISA.

The cell-culture supernatants at 10 days after HIV infection were examined for infectivity, and 10 days after HIV infection, cell supernatants were collected (termed HIV-1/Lenti cont and HIV-1/Lenti shNef366). CEMx174 CCR5/LTR-EGFP cells were infected with HIV-1/Lenti cont or HIV-1/Lenti shNef366, and the number of HIV-1-infected EGFP<sup>+</sup> T cells was determined by fluorescence-activated cell sorter (FACS).

#### Detection of chemokines

For the detection of chemokine production in MDMs, the cytometric bead array (CBA) kit (BD Bioscience, San Jose, CA) was used, which measured 4 chemokines (IL-8, MIP-1 $\alpha$ , MIP-1 $\beta$ , MCP-1) simultaneously.

#### Restimulation assay of lentivirus-transduced U1 cells

Latent HIV-1-infected U1 cells were transduced with Lenti cont or Lenti shNef366 at an MOI of 1. Two weeks later, EGFP<sup>+</sup> cells were sorted and stimulated with 1 ng/mL recombinant granulocyte-macrophage colony-stimulating factor (GM-CSF). Culture supernatants were collected at days 2 and 5, and the level of p24 antigen was measured by ELISA.

## Results

### siRNA suppresses *nef* mRNA and Nef protein expression

In the HIV-1 genome, *nef* is located at the 3' end of the viral genome, partially overlapping the 3' LTR (Figure 1A). Jacque and colleagues demonstrated previously that siRNA targeting of the 5' region of *nef* (nucleotides 164-185) suppressed HIV replication.<sup>20</sup> Therefore, we selected 3 distinct regions of the HIV-1<sub>NL432</sub> *nef* sequence using a Web-based program for designing DNA-directed RNAi systems, focusing on the Nef coding region overlapping the 3' LTR. These were designated as Nef338, 366, and 479 based on the position of the first nucleotide of the siRNA. From initial screening experiments, we found that Nef366 was the most effective target site (data not shown).

The type 1 interferon response is an innate defense mechanism in eukaryote cells against viral infection. It has been shown that some types of siRNA induce type 1 interferon, which in turn mediates the gene-specific effect of RNAi.<sup>21-23</sup> The stealth siRNA system was developed to avoid the interferon response to siRNA in cells (Invitrogen manual). We prepared synthetic stealth siRNAs, designated Nef355st and Nef366st, and a control siRNA designated

EGFPst, to determine the effect of RNAi using sequences based on Nef366 (the U3-overlapping region of the Nef-coding region). Nef355st was synthesized based on a Web-based computer program for generating stealth siRNA (Invitrogen), whereas Nef366st represents a slightly modified version of the stealth target site (6-nucleotide difference), so that it conformed to the target sequence as described. These stealth Nef siRNA sequences differed by only 5 nucleotides (Figure 1A).

We established a stable Nef-expressing HeLa-CD4 clonal cell line, designated as HeLa-CD4-Nef. HeLa-CD4-Nef cells were transfected either with 2.5  $\mu$ M EGFPst or *nef* stealth siRNAs (Nef355st or Nef366st), and harvested 48 hours after transfection. Total RNA was extracted and the level of *nef* mRNA was measured by qRT-PCR. We observed that transfection with Nef366st reduced *nef* mRNA expression more than 90% (Figure 1B), whereas Nef355st suppressed the level of *nef* mRNA approximately 80%, compared with EGFPst controls. When cell lysates of the transfected cells were analyzed by Western blot, we found that both Nef366st and Nef355st suppressed Nef protein levels to below the detection limit of the assay (Figure 1C). Taken together, these results clearly showed that Nef366 is an efficient target sequence for the inhibition of *nef* gene expression by siRNA.

### shRNA suppresses *nef* mRNA and Nef protein expression

To assess the effect of endogenous expression of Nef366 siRNA, we constructed expression vectors that encoded shRNAs corresponding to Nef366, or *lacZ* as a control, driven by the human U6 polymerase III promoter, designated as pENTR/shNef366 and pENTR/shLacZ, respectively (Figure 2A). HeLa-CD4-Nef cells were transfected with either pENTR/shNef366 or pENTR/shLacZ by FuGene6 reagent (Roche) and cells were harvested 72 hours after transfection. Total RNA was extracted and analyzed by qRT-PCR. We observed that the level of *nef* mRNA was suppressed by approximately 80% in cells transfected with pENTR/shNef366 (Figure 2B). Western blot analysis confirmed that pENTR/shNef366 strongly suppressed Nef protein levels as well (data not shown). These results indicated that promoter-driven endogenous

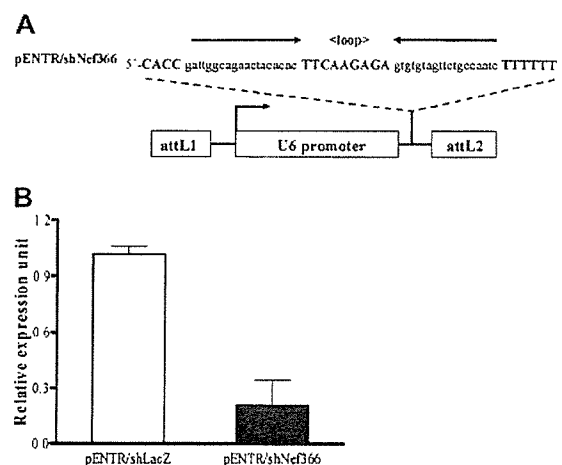


**Figure 2. RNAi by transfection with shRNA expression vectors.** (A) Schematic of the expression vectors (pENTR/shRNA) encoding shRNAs of Nef366 or *lacZ*, designated as pENTR/shNef366 and pENTR/shLacZ, respectively, in which expression is driven by the human U6 polymerase III promoter. (B) Nef-expressing HeLa-CD4 cells were transfected either with 1.0  $\mu$ g pENTR/shNef366 or pENTR/shLacZ and cells were harvested 72 hours after transfection. Total RNA was extracted and analyzed by qRT-PCR. The data represent the average  $\pm$  SD of 3 independent experiments.

expression of shNef366 was able to mediate RNAi of *nef* in HeLa-CD4-Nef cells.

#### Inhibition of HIV-1 replication in U937 cells by lentivirus-based shRNA expression

The transfection efficiency of the entry vectors used in suspension cells was quite low, and the objective here is to introduce siRNAs into primary macrophages. Therefore we constructed HIV-1–based lentivirus vectors expressing Nef366 shRNA or shRNA targeting lacZ as a control (Lenti shNef366 and Lenti control) using Gateway technology. The structure of the lentivirus vector used in the following studies is illustrated in Figure 3A.

To test whether Nef366 shRNA was able to efficiently block HIV-1 replication, we infected U937 cells with Lenti shNef366 or Lenti control, both of which encoded GFP driven by the EF1 $\alpha$  promoter (EGFP), at an MOI of 1. Two weeks after infection, nearly 30% of the cells stably expressed EGFP (Figure 3B upper panel). We sorted the EGFP<sup>+</sup> cells by fluorescence-activated cell sorter (FACSaria; BD Biosciences), after which the purity of the Lenti control– and Lenti shNef366–transfected, EGFP<sup>+</sup> cells was 97.2% and 99.7%, respectively (Figure 3B lower panel; U937/Lenti cont and U937/Lenti shNef366). The purified cell populations were then infected with 2 inoculation doses of HIV-1 (Figure 3C upper and lower panels; p24: 20 ng and 100 ng, respectively). The culture supernatants were collected at 3- or 4-day intervals, and the level of p24 antigen was measured by ELISA. We observed that at both inoculation doses HIV-1 replication in U937 cells was inhibited by Lenti shNef366, especially at the peak of HIV-1

production. The reverse transcriptase activity was also measured in parallel, and the result was consistent with that of p24 ELISA (data not shown). The inhibition of HIV-1 replication was sustained at least for 1 week, following which HIV-1 production gradually decreased in all cell populations, presumably because of the cytopathic effect of HIV-1 infection.

To further evaluate the effect of RNAi on the early steps of HIV-1 infection, we prepared cell lysates at different time points after inoculation (3, 8, and 12 hours after infection) and analyzed the level of reverse transcription activity by measuring the amount of different forms of proviral DNA (HIV-1 *2LTR* and *U5-Gag*) by the qRT-PCR. The copy number of these proviral DNA forms decreased in U937/Lenti shNef366 cells, relative to that seen in U937/Lenti control cells at all time points. The amount of these DNA forms normalized to  $\beta$ -globin gene at 12 hours after HIV-1 infection is depicted in Figure 3D. The copy number of *2LTR* and *U5-Gag* was 16.9% and 13.4% of control, respectively. These results suggested that the inhibition of HIV-1 replication occurred early after virus entry, presumably during uncoating or reverse transcription, not integration.

A type I interferon response has been shown to be induced by synthetic siRNAs via protein kinase R- (PKR) or toll-like receptor 7 (TLR 7)–mediated signaling pathways.<sup>21–23</sup> To eliminate the possibility that we were generating an interferon response following shRNA expression in our system, we analyzed the level of 2' 5'-oligoadenylate synthetase mRNA expression in Lenti shNef366–infected U937 cells by qRT-PCR. We detected no such message (data not shown), indicating that the interferon response plays a

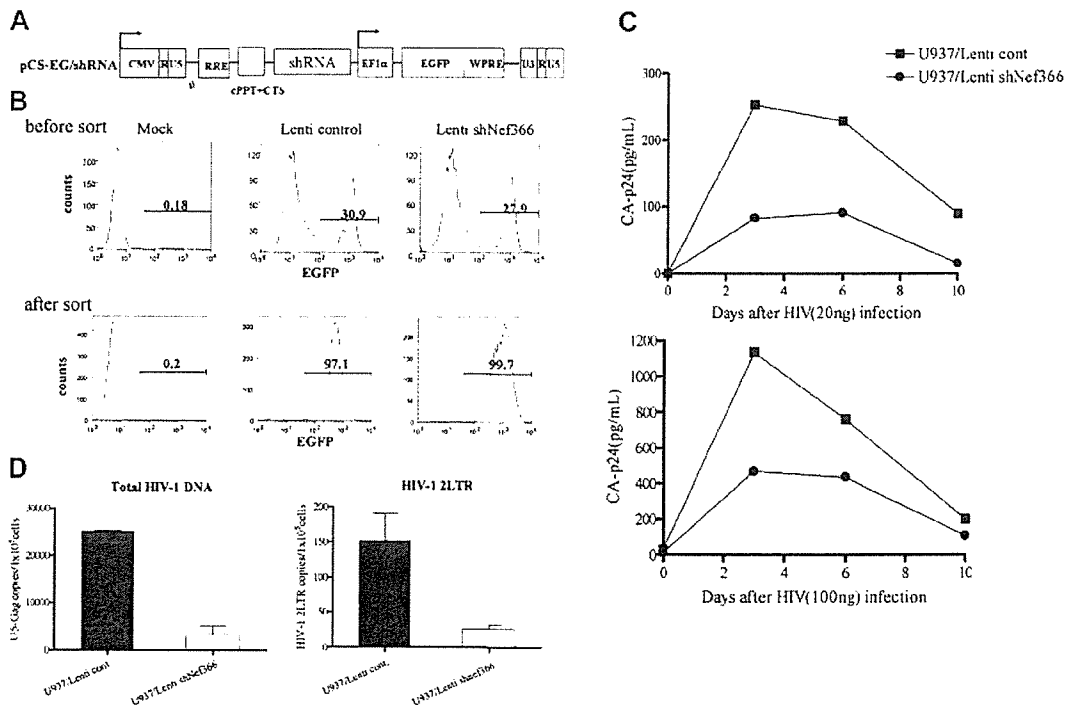


**Figure 3.** Inhibition of HIV-1 replication in U937 cells by lentivirus-mediated shRNA. (A) The structure of the shRNA lentiviral expression vector. The HIV-1–based lentivirus vector for expressing shRNA was constructed using Gateway technology. pCS-EG/shRNA consisted of U6-shRNA upstream of an EF1 $\alpha$  promoter–driven EGFP expression cassette, which allowed simultaneous expression of shRNA and EGFP. (B) U937 cells were infected with lentivirus expressing either shNef366 (Lenti shNef366) or shLacZ (Lenti control) at an MOI of 1. After 2 hours of infection, cells were washed and maintained in culture. Cells expressing EGFP were analyzed by FACS, and EGFP<sup>+</sup> cells were collected. EGFP<sup>+</sup> cells were analyzed by FACSaria 1 week later (designated as U937/Lenti control and U937/Lenti shNef366). (C) U937/Lenti cont or U937/Lenti shNef366 cells ( $1 \times 10^6$ /well) were infected with HIV-1<sub>NI\_432</sub>, and the culture supernatants of these cells were collected at 3- or 4-day intervals after infection. The level of p24 antigen in the culture supernatants was measured by ELISA. (D) HIV-1–infected cells were collected and total DNA was prepared 12 hours after infection. Total HIV-1 and 2LTR DNA was analyzed by qRT-PCR. The amount of HIV-1–specific DNA per cell was normalized to  $\beta$ -globin gene expression. The data represent the average  $\pm$  SD of 3 independent experiments.



minimal role, if any, in the observed inhibitory effect on HIV replication by Lenti shNef366.

#### Lentivirus-based nef shRNA inhibits HIV-1 replication and affects chemokine production in MDMs

Swingler and coworkers reported that HIV-1 Nef expression in macrophages mediated lymphocyte chemotaxis and activation through the induction of MIP-1 $\alpha$  and MIP-1 $\beta$  expression.<sup>8</sup> To determine the effect of Nef expression during HIV-1 infection in MDMs, we infected MDMs with wild-type HIV-1<sub>NF462</sub> or the corresponding *nef* gene-deletion mutant, HIV-1<sub>NF462</sub>dNef, and assessed the kinetics of virus replication by p24-specific ELISA. Representative results from 2 donors are shown in Figure 4A. We consistently observed that the level of HIV-1<sub>NF462</sub> replication was 2- to 6-fold higher than that of HIV-1<sub>NF462</sub>dNef in MDMs. These results were consistent with those reported by Swingler et al.<sup>9</sup> Although no apparent T-cell damage was observed during cultivation for 3 weeks following HIV-1 infection, the amount of virus production gradually decreased. We analyzed chemokine production in MDMs infected with HIV-1 wild-type and *nef*-deleted HIV-1 at days 10, 14, and 17 after infection. The level of chemokine production in uninfected MDMs varied depending on the donor, but both donors produced a high level of IL-8 and monocyte chemoattractant protein-1 (MCP-1), and a low level of MIP-1 $\alpha$  and MIP-1 $\beta$  (data not shown). HIV infection per se, independent of the presence or absence of Nef, did not affect this trend, in that the levels of these chemokines, with the exception of MIP-1 $\beta$ , were only slightly affected by HIV infection. Notably, virus replication resulted in an increased production of MIP-1 $\beta$ , which peaked at 14 days after infection, in parallel with the peak of viral replication. Figure 4B shows the results of the analysis of the levels of MIP-1 $\beta$  and MIP-1 $\alpha$  in the 2 donors. HIV-1 infection induced a 2-fold increase in the level of MIP-1 $\beta$  compared with mock-infected MDMs. In contrast, infection with *nef*-deleted HIV-1 caused a reduction in the level of MIP-1 $\beta$  in the MDMs from both donors, indicating that Nef is responsible for the up-regulation of MIP-1 $\beta$ , but does not affect MIP-1 $\alpha$ , MCP-1, or IL-8 production.

To examine whether shRNAs against the U3-overlapping region of *nef* were able to block HIV-1 replication in MDMs, we infected MDMs with Lenti control or Lenti shNef366, at an MOI of 10 or 2 (Figure 5A left and right panels, respectively). After 2 hours of incubation, cells were extensively washed and cultivated overnight, and the following day, they were infected with HIV-1<sub>NF462</sub>. Culture supernatants were collected every 3 or 4 days and

the level of p24 antigen was measured by ELISA. Of note, despite the extensive washing after lentivirus infection, the level of p24 was quite high up to 7 days after HIV-1 infection. We detected a second peak of virus production, which we interpreted as true HIV-1 replication in MDMs transduced with lentiviral vectors expressing shRNAs. In addition, presumably because of the toxic effect of infection by lentivirus pseudotyped with VSV, the level of p24 antigen was lower than that in MDMs infected with HIV-1 virus. Nevertheless, we observed a similar level of inhibition of HIV-1 replication in MDMs by Lenti shNef366 at 2 different doses of infection (Figure 5A), and the inhibition was maintained for at least 3 weeks after HIV-1 infection.

Macrophages can mediate efficient infection of lymphocytes *in trans*,<sup>9,24</sup> suggesting that macrophages serve as a major reservoir and vehicle for HIV-1 dissemination. We were interested in whether the progeny virus produced from MDMs harboring Nef366 shRNA maintained their ability to infect T cells. Supernatants from MDM cells transduced with Lenti control or Lenti shNef366 were collected 10 days after HIV infection, and the level of p24 antigen was measured and used to quantitate the amount of HIV present. These sources of HIV were designated as HIV/Lenti cont or HIV/Lenti shNef366. Using CEMx174 CCR5/LTR-EGFP cells as indicator cells, we estimated the infectivity of HIV/Lenti cont or HIV/Lenti shNef366 by analyzing the number of EGFP<sup>+</sup> T cells following infection (Figure 5B). Compared with HIV-1/Lenti cont, HIV-1/Lenti shNef366 had a significant loss of infectivity in CCR5<sup>+</sup> T cells. Our results suggested that Lenti shNef366 has the potential to protect HIV-1 dissemination to T cells by HIV-1-infected MDMs.

We also examined the level of chemokine production following HIV infection of MDMs transduced with shRNA lentivirus vectors. Although the basal level of MIP-1 $\alpha$  and MIP-1 $\beta$  production was slightly increased following lentivirus infection, the level of MIP-1 $\beta$  decreased in Lenti shNef366 cells compared with Lenti control (Figure 5C). The levels of MCP-1 and IL-8 were either unaffected or somewhat restored by Lenti shNef366 (data not shown).

#### Lentivirus-based nef shRNA protects progression from latent HIV-1 infection to productive infection

Latent HIV-1 infection can be established following provirus integration into the host genome.<sup>25-27</sup> A small number of infected cells re-enter the resting stage, harboring an integrated copy of the HIV-1 genome. These latent HIV-infected cells represent a barrier to successful virus eradication because subsequent cytokine or

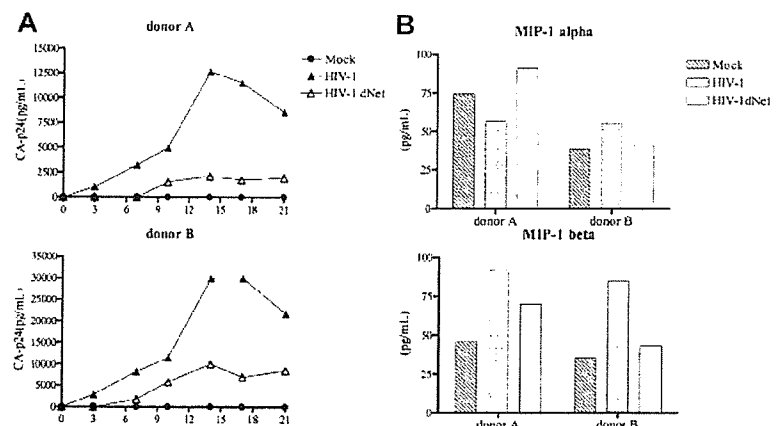


**Figure 4.** The effect of Nef expression during HIV-1 infection in MDMs. (A) MDMs ( $2 \times 10^6$ /well) of 2 donors were infected either with wild-type HIV-1<sub>NF462</sub> or HIV-1<sub>NF462</sub>dNef. The supernatants of these wells were harvested at 3- or 4-day intervals after infection, and viral production was monitored by sequential quantitation of p24 by ELISA. (B) The CBA kit was used to measure the level of chemokines (MIP-1 $\alpha$  and MIP-1 $\beta$ ) in cell supernatants 14 days after HIV infection.

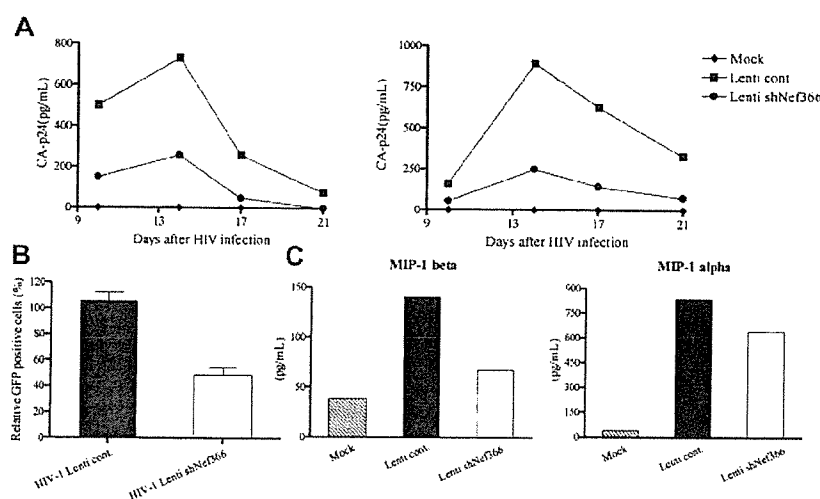


**Figure 5. Lentivirus-expressed nef shRNA inhibits HIV-1 replication and affects chemokine production in MDMs.** (A) MDMs were transduced with Lenti cont or Lenti shNef366 at an MOI of 2. At 2 hours after infection, cells were washed twice, then cultured for another 24 hours, at which point the cells were infected with HIV-1<sub>NF-462</sub>. The culture supernatants were collected at 3- or 4-day intervals after HIV infection, and the level of p24 antigen was measured by ELISA. (B) MDMs transduced either with Lenti control or Lenti shNef366 were infected with HIV-1 and supernatants were collected 10 days after infection and designated as HIV-1 Lenti cont and HIV-1 Lenti shNef366, respectively. CEMx174 CCR5/LTR-EGFP cells were infected either with HIV-1 Lenti cont or HIV-1 Lenti shNef366 and GFP<sup>+</sup>, HIV-1-infected T cells were analyzed by FACS 48 hours later. The data represent the average  $\pm$  SD of 3 independent experiments. (C) The culture supernatants of MDMs transduced with lentivirus vectors were collected 14 days after infection and the levels of the chemokines MIP-1 $\alpha$  and MIP-1 $\beta$  were measured.

other stimuli can reactivate viral gene expression, and reinitiate HIV-1 replication.<sup>28-31</sup> We were interested in whether Lenti shNef366 was able to regulate the progression of latent HIV-1 infection to productive infection in U1 cells.<sup>17</sup> U1 cells are U937 cells in which a latent HIV-infection has been established, and HIV-1 replication can be induced in these cells on appropriate activation. We transduced U1 cells with Lenti control or Lenti shNef366 at an MOI of 1. After 2 hours of infection, cells were extensively washed and maintained in culture. Two weeks after transduction, the cells were sorted by FACSaria, and the EGFP<sup>+</sup> cell population was stimulated with 1 ng/mL recombinant GM-CSF. Culture supernatants were collected at different time points (days 2 and 5) and the level of p24 antigen was measured by ELISA. As shown in Figure 6, the levels of p24 antigen were dramatically decreased in U1 cells harboring Lenti shNef366 at all time points examined.

## Discussion

In this study, we constructed an shRNA expression system that targeted HIV *nef* gene sequences that overlap the 3' LTR U3 (Nef366) and showed that Nef366 shRNA had a strong inhibitory effect on *nef* gene expression in Nef-expressing HeLa-CD4 cells. Furthermore, expression of shNef366 in monocytic cell lines strongly inhibited the replication of HIV-1 at an early stage of HIV

infection. The rationale for using shNef366 to target HIV *nef* was several-fold. Because the U3 region is required during reverse transcription for first template transfer and integration of the viral genome into the host genome, siRNA targeting of the U3 region may induce not only specific degradation of *nef* mRNA, but also inhibit HIV-1 reverse transcription. Furthermore, although others have observed escape mutations in RNAi experiments targeting *nef* or *tat*,<sup>32,33</sup> the *nef*/U3 sequence we targeted is highly conserved as discussed in the paragraph after the next one. If a mutation were to occur in the U3 region, it would affect the overall transcription efficiency of HIV-1 after integration because the U3 region of the HIV-1 LTR contains the transcription initiation or promoter/enhancer sites that are essential for efficient HIV transcription. Of note, the strategy used Jacque et al<sup>20</sup> using siRNA targeting of the 5' region of *nef* turned out to induce an escape mutant.<sup>33</sup> Although we did not extensively test for the emergence of escape mutants, targeting the 3' LTR U3-overlapping region of *nef* (Nef366) represented a potentially potent strategy for controlling HIV-1 replication.

Macrophages are one of the major target cell populations in the early phase of HIV-1 infection, when R5 viruses predominate.<sup>34</sup> HIV-1 replication in macrophages is usually slow and less cytopathic compared with that in activated T cells, allowing the virus to survive long after infection. Thus, macrophages serve as one of the reservoirs for HIV in an infected individual.<sup>35</sup> Therefore, therapeutic strategies that target macrophages are promising approaches to the control of persistent HIV-1 infection in vivo. Taking advantage of the lentivirus expression system, which is an efficient way to introduce a desired gene into primary cells, we were able to show that expression of Nef366 shRNAs in primary MDMs inhibited HIV-1 replication in these cells.

In this context, several groups have demonstrated that RNAi, mediated by the introduction of HIV-specific siRNA duplexes, can inhibit viral replication in T cells, although the effect was transient.<sup>20,36-38</sup> Das et al were able to show a stable inhibitory effect on viral replication using a murine retrovirus vector expressing Nef-specific siRNAs in T-cell lines. However, the block in virus replication was not absolute and escape mutants emerged.<sup>33</sup> These previous results prompted us to develop a novel strategy of RNAi-mediated inhibition of HIV infection that did not induce a type I interferon and had a stable, long-term effect. We chose to

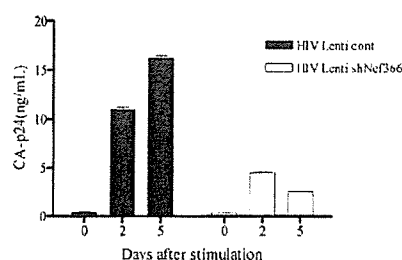


**Figure 6. The effect of Lenti shNef366 on latent HIV-1 infection.** Latent HIV-1-infected U1 cells were transduced with Lenti control or Lenti shNef366 at an MOI of 1. Two weeks after infection, EGFP<sup>+</sup> cells were sorted by FACSaria, and EGFP<sup>+</sup> cells were stimulated with 1 ng/mL recombinant GM-CSF. Cell-culture supernatants were collected 0, 2, and 5 days after stimulation, and the level of p24 antigen was measured by ELISA. The data represent the averages  $\pm$  SDs of 3 independent experiments.

transduce Nef366 shRNA into low or nondividing primary macrophages, as opposed to actively proliferating T cells, using a lentivirus expression vector, and were able to demonstrate RNAi effect during macrophage cultivation for 3 weeks. Using an alignment of 200 HIV-1 sequences obtained by BLAST search analysis, only one base mismatch in the Nef366 region was detected in a subtype A virus (GenBank no. AB098332 and no. AB098333, HIV-1 UG029). Further study will be required to determine whether this subtype A virus is resistant to shRNA Nef366. Because Nef/LTR is in a completely conserved region, at least among subtype B viruses, this region might have quite an important function for HIV-1 replication. We speculate that if escape mutants were to emerge in the presence of lentiviral-shRNA Nef366, the compensatory mutation would occur outside of this region.

Importantly, using this system, we were also able to demonstrate a decrease in the infectivity of HIV-1 produced from infected MDMs. This attenuation effect is potentially significant because it implies that lentivirus-mediated RNAi may also reduce transmissibility of HIV-1 overall. However, in light of the significant problem of viral escape during chronic HIV infection, it may become necessary to combine multiple sites of siRNAs targeting the *nef-U3* region in the future.

Control of the latent phase of HIV infection is a key issue for effective therapeutic intervention. We demonstrated here that Lenti shNef366 was able to suppress the reactivation of HIV from latently infected cells. The expression of integrated HIV-1 in latently infected cells is controlled at the level of transcription by cellular factors and the viral transactivator Tat, both of which act through the HIV-1 LTR.<sup>39</sup> Transcription of integrated viral RNA is initiated at the R region of the 5' LTR. The fact that shNef366, which targeted the U3-overlapping region of Nef, was effective in latently infected cells, suggests that shNef366 can directly target cleavage of *nef* mRNAs or total viral RNAs at the 3' end. Therefore, our lentivirus-based shRNA expression system appears to be able to control both early and latent HIV-1 infection.

MIP-1 $\alpha$  and MIP-1 $\beta$  are ligands of the HIV-1 coreceptor, CCR5. Through interaction with the CCR5 receptor, they promote

the maturation of Th1 cells.<sup>40,41</sup> Swingler et al reported that MIP-1 $\alpha$  and MIP-1 $\beta$  were induced by Nef in macrophages during HIV infection and that culture supernatants derived from Nef-expressing macrophages induced both chemotaxis and activation of resting T lymphocytes, enabling productive HIV-1 infection of those T cells.<sup>8</sup> These and other results have led to a model of HIV infection in which expression of Nef in HIV-infected MDMs enhances the secretion of MIP-1 $\beta$ , which recruits mainly CCR5<sup>+</sup> Th1 cells, resulting in the expansion of R5 tropic HIV-1 during macrophage-T-cell interactions. Our results were partially consistent with this model because the degradation of *nef* mRNA expression resulted in the decreased MIP-1 $\beta$  production. Of note, the production of MIP-1 $\alpha$  in our system appeared to be unaffected by Nef expression but was induced by lentivirus infection. Because the production of MIP-1 $\alpha$  in HIV-infected MDMs was similar to that in uninfected MDMs, it seems likely that MIP-1 $\alpha$  production was enhanced by a non-HIV-specific component of the lentivirus expression system, perhaps VSV-G protein. Although the levels of MCP-1 and IL-8 varied depending on the donor and were independent of Nef expression, we cannot rule out the possibility that other unknown chemokines are induced by Nef. Any such dysregulated chemokine production by Nef expression in macrophages might provide an appropriate environment for HIV to establish an efficient infection and dissemination.

In summary, we demonstrated the feasibility of using lentiviral expression vectors to express shRNAs against the U3-overlapping region of *nef* in primary MDMs, as a type of intracellular immunization and potential gene therapy approach against HIV-1. Future development of an AIDS vaccine based on the specific inhibition of viral gene expression combined with existing therapeutic strategies may provide keys to help eradicate HIV.

## Acknowledgments

We thank Masayuki Ishige and Rieko Iwaki for their excellent technical assistance.

## References

- Kestler HW 3rd, Ringler DJ, Mori K, et al. Importance of the *nef* gene for maintenance of high virus loads and for development of AIDS. *Cell*. 1991;65:651-662.
- Agopian K, Wei BL, Garcia JV, Gabuzda D. A hydrophobic binding surface on the human immunodeficiency virus type 1 Nef core is critical for association with p21-activated kinase 2. *J Virol*. 2006;80:3050-3061.
- Fackler OT, Baur AS. Live and let die: Nef functions beyond HIV replication. *Immunity*. 2002;16:493-497.
- Geyer M, Fackler OT, Peterlin BM. Structure-function relationships in HIV-1 Nef. *EMBO Rep*. 2001;2:580-585.
- Steffens CM, Hope TJ. Recent advances in the understanding of HIV accessory protein function. *AIDS*. 2001;15(suppl 5):S21-S26.
- Na YS, Yoon K, Nam JG, et al. Nef from a primary isolate of human immunodeficiency virus type 1 lacking the EE(155) region shows decreased ability to down-regulate CD4. *J Gen Virol*. 2004;85:1451-1461.
- Deacon NJ, Tsykin A, Solomon A, et al. Genomic structure of an attenuated quasi species of HIV-1 from a blood transfusion donor and recipients. *Science*. 1995;270:988-991.
- Swingler S, Mann A, Jacque J, et al. HIV-1 Nef mediates lymphocyte chemotaxis and activation by infected macrophages. *Nat Med*. 1999;5:997-1003.
- Swingler S, Brichacek B, Jacque JM, Ulrich C, Zhou J, Stevenson M. HIV-1 Nef intersects the macrophage CD40L signalling pathway to promote resting-cell infection. *Nature*. 2003;424:213-219.
- Hannon GJ. RNA interference. *Nature*. 2002;418:244-251.
- Coburn GA, Cullen BR. Potent and specific inhibition of human immunodeficiency virus type 1 replication by RNA interference. *J Virol*. 2002;76:9225-9231.
- Lee MT, Coburn GA, McClure MO, Cullen BR. Inhibition of human immunodeficiency virus type 1 replication in primary macrophages by using Tat- or CCR5-specific small interfering RNAs expressed from a lentivirus vector. *J Virol*. 2003;77:11964-11972.
- Novina CD, Murray MF, Dykxhoorn DM, et al. siRNA-directed inhibition of HIV-1 infection. *Nat Med*. 2002;8:681-686.
- Qin XF, An DS, Chen IS, Baltimore D. Inhibiting HIV-1 infection in human T cells by lentiviral-mediated delivery of small interfering RNA against CCR5. *Proc Natl Acad Sci U S A*. 2003;100:183-188.
- Song E, Lee SK, Dykxhoorn DM, et al. Sustained small interfering RNA-mediated human immunodeficiency virus type 1 inhibition in primary macrophages. *J Virol*. 2003;77:7174-7181.
- Miyoshi H, Blomer U, Takahashi M, Gage FH, Verma IM. Development of a self-inactivating lentivirus vector. *J Virol*. 1998;72:8150-8157.
- Folks TM, Justement J, Kinter A, Dinarello CA, Fauci AS. Cytokine-induced expression of HIV-1 in a chronically infected promonocyte cell line. *Science*. 1987;238:800-802.
- Tsunetsugu-Yokota Y, Kato T, Yasuda S, et al. Transcriptional regulation of HIV-1 LTR during antigen-dependent activation of primary T cells by dendritic cells. *J Leukoc Biol*. 2000;67:432-440.
- Yamamoto N, Tanaka C, Wu Y, et al. Analysis of human immunodeficiency virus type 1 integration by using a specific, sensitive and quantitative assay based on real-time polymerase chain reaction. *Virus Genes*. 2006;32:105-113.
- Jacque JM, Triques K, Stevenson M. Modulation of HIV-1 replication by RNA interference. *Nature*. 2002;418:435-438.
- Hornung V, Guenther-Biller M, Bourquin C, et al. Sequence-specific potent induction of IFN- $\alpha$  by short interfering RNA in plasmacytoid dendritic cells through TLR7. *Nat Med*. 2005;11:263-270.
- Bridge AJ, Pebernard S, Ducraux A, Nicolaz AL,

- Iggo R. Induction of an interferon response by RNAi vectors in mammalian cells. *Nat Genet*. 2003;34:263-264.
23. Sledz CA, Holko M, de Veer MJ, Silverman RH, Williams BR. Activation of the interferon system by short-interfering RNAs. *Nat Cell Biol*. 2003;5:834-839.
24. Carr JM, Hocking H, Li P, Burrell CJ. Rapid and efficient cell-to-cell transmission of human immunodeficiency virus infection from monocyte-derived macrophages to peripheral blood lymphocytes. *Virology*. 1999;265:319-329.
25. Garcia-Blanco MA, Cullen BR. Molecular basis of latency in pathogenic human viruses. *Science*. 1991;254:815-820.
26. McCune JM. Viral latency in HIV disease. *Cell*. 1995;82:183-188.
27. Finzi D, Siliciano RF. Viral dynamics in HIV-1 infection. *Cell*. 1998;93:665-671.
28. Chun TW, Stuyver L, Mizell SB, et al. Presence of an inducible HIV-1 latent reservoir during highly active antiretroviral therapy. *Proc Natl Acad Sci U S A*. 1997;94:13193-13197.
29. Finzi D, Hermankova M, Pierson T, et al. Identification of a reservoir for HIV-1 in patients on highly active antiretroviral therapy. *Science*. 1997;278:1295-1300.
30. Wong JK, Hezareh M, Gunthard HF, et al. Recovery of replication-competent HIV despite prolonged suppression of plasma viremia. *Science*. 1997;278:1291-1295.
31. Chun TW, Engel D, Mizell SB, Ehler LA, Fanci AS. Induction of HIV-1 replication in latently infected CD4<sup>+</sup> T cells using a combination of cytokines. *J Exp Med*. 1998;188:83-91.
32. Boden D, Pusch O, Lee F, Tucker L, Ramratnam B. Human immunodeficiency virus type 1 escape from RNA interference. *J Virol*. 2003;77:11531-11535.
33. Das AT, Brummelkamp TR, Westerhout EM, et al. Human immunodeficiency virus type 1 escapes from RNA interference-mediated inhibition. *J Virol*. 2004;78:2601-2605.
34. Moore JP, Kitchen SG, Pugach P, Zack JA. The CCR5 and CXCR4 coreceptors—central to understanding the transmission and pathogenesis of human immunodeficiency virus type 1 infection. *AIDS Res Hum Retroviruses*. 2004;20:111-126.
35. Aquaro S, Calio R, Balzarini J, Bellocchi MC, Garaci E, Perno CF. Macrophages and HIV infection: therapeutical approaches toward this strategic virus reservoir. *Antiviral Res*. 2002;55:209-225.
36. Capodici J, Kariko K, Weissman D. Inhibition of HIV-1 infection by small interfering RNA-mediated RNA interference. *J Immunol*. 2002;169:5196-5201.
37. Dave RS, Pomerantz RJ. Antiviral effects of human immunodeficiency virus type 1-specific small interfering RNAs against targets conserved in select neurotropic viral strains. *J Virol*. 2004;78:13687-13696.
38. Stevenson M. Dissecting HIV-1 through RNA interference. *Nat Rev Immunol*. 2003;3:851-858.
39. Cullen BR. HIV-1 auxiliary proteins: making connections in a dying cell. *Cell*. 1998;93:685-692.
40. Loetscher P, Ugucioni M, Bordoli L, et al. CCR5 is characteristic of Th1 lymphocytes. *Nature*. 1998;391:344-345.
41. Luther SA, Cyster JG. Chemokines as regulators of T cell differentiation. *Nat Immunol*. 2001;2:102-107.